Sexually Dimorphic Influence of Circadian Pacemaker Neurons on Behavioral Rhythms

Aishwarya Ramakrishnan Iyer[1,2], Eva Scholz-Carlson[1,2], Evardra Bell[2], Grace Biondi[2], Shlesha Richhariya[3], and Maria P. Fernandez[1,2,*]

1- Department of Biology, Indiana University Bloomington. Bloomington, IN
2- Department of Neuroscience and Behavior, Barnard College. New York City, NY
3- HHMI, Brandeis University. Waltham, MA

*Corresponding author: fernanm@iu.edu

Abstract

The circadian system regulates the timing of multiple molecular, physiological, metabolic, and behavioral phenomena. In *Drosophila*, as in other species, most of the research on how the timekeeping system in the brain controls the timing of behavioral outputs has been conducted in males, or sex has not been included as a biological variable. A critical set of circadian pacemaker neurons in *Drosophila* release the neuropeptide pigment-dispersing factor (PDF), which functions as a key output factor in the network with complex effects on other clock neurons. Lack of *Pdf* or its receptor, *PdfR*, results in most flies displaying arrhythmicity in activity–rest cycles under constant conditions. However, our results show that female circadian rhythms are less affected by mutations in both *Pdf* and *PdfR*. Crispr-Cas9-mediated mutagenesis of *Pdf*, specifically in ventral lateral neurons (LN_vs), also has a greater effect on male rhythms. We tested the influence of M-cells on the circadian network and showed that speeding up the molecular clock specifically in M-cells led to sexually dimorphic phenotypes, with a more pronounced effect on male rhythmic behavior. Our results suggest that the female circadian system is more resilient to manipulations of M-cells and the PDF pathway, suggesting that circadian timekeeping is more distributed across the clock neuron network in females.

Keywords: circadian rhythms, sex differences, PDF, *Drosophila*, sleep/wake cycles, oscillator hierarchies

Introduction

Differences in neuronal circadian timekeeping between sexes remain relatively unexplored, despite the expanding body of research highlighting the influence of sex on the mechanisms underlying neuronal control of behavior [1]. In mammals, steroid hormones display daily, clock-driven changes in abundance, and while these sex hormones are not required to maintain rhythms, they differentially influence the amplitude of activity behavior between the sexes [1, 2]. Furthermore, structural and functional sex differences have been observed in brain areas that receive direct input from the brain's circadian timekeeping center [2, 3]. Research in humans has also revealed significant sexual dimorphism: men tend to have lower-amplitude endogenous rhythms than women [4], are less resilient to nocturnal sleep disruptions, and spend less time asleep [5].

In mammals, the main circadian pacemaker resides in the suprachiasmatic nuclei (SCN), which in mice consist of a network of ~20,000 neurons (reviewed in [6]). The *Drosophila* circadian clock network has ~150 neurons and is the functional equivalent of the mammalian SCN [7, 8]. Each circadian clock neuron has an intracellular molecular timekeeping mechanism based on a transcriptional□translational feedback loop: the genes *Clock* (*Clk*) and *cycle* (*cyc*) promote rhythmic transcription of several key genes, including *Period* (*Per*) *and Timeless* (*Tim*), which build up daily and inhibit their own transcription [9]. Multiple kinases that act on components of these clock proteins and can affect the pace of the molecular clock have been identified. One such kinase is *Doubletime* (DBT), which binds to and phosphorylates PER, regulating its nuclear accumulation [10, 11].

The fly clock network consists of *lateral neurons (LNs*), which include ventrolateral (LN_v), dorsolateral (LN_d), and lateral posterior neurons (LPNs), as well as three groups of *dorsal neurons* (*DN1, DN2, and DN3*), some of which can be further subdivided [8, 12-15]. The ventral and dorsal LNs are sufficient to produce the normal endogenous bimodal rhythm of sleep and activity [16, 17]. The four small LN_vs (s-LN_vs) are usually referred to as morning cells (M-cells) since they control the morning peak of activity under light□dark cycles (LDs). These cells are also essential for maintaining rhythmicity under free-running conditions [18, 19]. The evening peak is controlled by the LN_ds and a *Pdf*-negative LN_v, the 5th LN_v (E-cells) [16, 20, 21]. Some

DNs also contribute to the timing and amount of sleep via the modulation of M and E cells [22-25].

The release of the circadian neuropeptide Pigment Dispersing Factor (PDF) by s-LN_vs is essential for endogenous circadian timekeeping. A *Pdf* null mutation, Pdf^{01}, results in a substantial fraction of arrhythmic flies [18], desynchronization of molecular oscillations [26, 27], and phase changes in the electrical activity of some clock clusters, most notably the LN_ds [28]. Loss of *PdfR* also leads to loss of behavioral rhythms [29-31]. Interestingly, PDF and PDFR also regulate behaviors that are sex-specific or sexually dimorphic. Rival-induced long mating durations require PDF expression in s-LN_vs, PDFR expression in a subset of LN_ds, and NPF expression in LN_ds [32]. PDF controls rhythms in the sexually dimorphic pheromone profiles produced by oenocytes [33] and is involved in long-term mating suppression in males [34]. Both PDF and PDFR contribute to geotactic behaviors [29], and the phenotypes of Pdf^{01} mutants are sexually dimorphic, with males showing a more extreme negative geotaxis phenotype [35].

Sexual dimorphism in *Drosophila* sleep/wake cycles has been studied mostly under LD cycles. Males exhibit lower levels of activity and more sleep during the light phase [36-38]. This increase in midday sleep is due to the activity of a subset of sleep-promoting DN1s, which are more active in males [36] and receive input from the male-specific P1 neurons that control male courtship [37]. Unlike studies on circadian rhythms, *Drosophila* sleep research often involves only females. Males also have an earlier and more pronounced morning peak and a larger phase angle between the morning peak and the evening peak [39]. Under conditions of constant darkness and temperature (DD), males of several wild-type strains have a small but significant reduction in the free-running period (FRP) relative to females of the same strain [39]. Moreover, males are more likely to retain a bimodal activity pattern in DD [39]. A recent transcriptomic analysis of *fruitless* (*fru*)-expressing neurons revealed clusters that are enriched for circadian clock genes [40]. Interestingly, only the male dataset revealed coexpression of *fru*- and circadian-related genes. A previous study reported that DN1s express the male-specific Fru^M protein [41] and that the number of cells in the $DN1_p$s cluster is sexually dimorphic [42]. In addition, the E3 subset of LN_ds has been shown to be dimorphic in its expression of the neuropeptide NPF [43, 44].

Given the sexually dimorphic roles of neuropeptides, including PDF, in other behaviors [45], we asked whether females were similarly affected by manipulations of the *Pdf/PdfR* pathway. We found that female circadian rhythms are less affected by null mutations in both *Pdf* and *PdfR* and that similar effects are observed via CRISPR-Cas9-mediated *Pdf* mutagenesis, specifically in the LN_vs. Moreover, speeding up the molecular clock in the LN_vs via expression of DBT^s leads to an advance of the morning peak in males but not in females, and the pace of the free-running period of activity is significantly shortened only in males. Taken together, our results show that the female circadian system is more resilient to manipulations in the PDF pathway and suggest that *Pdf*+ neurons play a more dominant role in the male than in the female circadian network.

Results

Mutations in PDF and PDFR lead to sexually dimorphic phenotypes.

A null mutation in *Pdf* results in pronounced behavioral phenotypes in *Drosophila* males [18]. We assayed the locomotor activity rhythms of Pdf^{01} females under free-running conditions (DD) and found that a large proportion of the experimental females were still rhythmic (Fig. 1 A-C). The rhythmic power of experimental flies was significantly reduced in both sexes (Fig. 1D), but the effect was less pronounced in females (Fig. 1E), suggesting that Pdf^{01} females have more consolidated rhythms than Pdf^{01} males. Mutant females that were rhythmic had a slightly, but significantly, shorter free-running period than the controls (Table 1). This phenotype was not always observed in experimental males (Table 1), consistent with a recent study [46]. Sleep cycles under DD also appeared to be more consolidated in females (Fig. 1F). *Pdf* mutants have increased sleep, and this effect is mediated by PDF acting on the LN_vs themselves [47]. We found that both sexes show an increase in total sleep in LD, but the effect was more pronounced in females (Fig. 1G-I). While the increase in sleep in males was most prominent at midday, females exhibited increased sleep throughout most of the light phase (Fig. 1G).

To rule out the presence of remnant PDF expression in Pdf^{01} females, we stained the brains of control and experimental males and females with an anti-PDF antibody. We did not observe any

traces of PDF in experimental flies of either sex, even with increased laser intensity (Fig. S1A). PDF accumulates rhythmically in the dorsal termini of the s-LN_v projections in a time-of-day-dependent manner both in LD and DD [18, 19]. To determine if there were differences in the amplitude of PDF cycling between the sexes in a wild-type background (Canton-S), we dissected control males and females on the third day under DD at 6 timepoints over a 24-hour cycle. Using a COSINOR-based curve fitting method [48], we found that both males and females have clear 24-hour rhythms in PDF cycling in their dorsal projections, with no significant sex differences in amplitude (Fig. S1B-C, Table 2).

Next, we asked whether the effects of a *Pdf* receptor mutation (*PdfR*) on activity and sleep were also sexually dimorphic. The expression of PDFR, a GPCR, can be detected in most clock neurons, with the exception of 3 LNds, half DN1ps, and some DN3s [49], which coincides with *Cryptochrome* expression in clock neurons [49]. The han^{5304} mutant is a *PdfR* hypomorph and exhibits Pdf^{01}-like behavioral phenotypes under both LD 12:12 and DD [29-31]. Under DD, both *Han* males and females showed a significant reduction in rhythmicity compared with the controls, but there was a greater proportion of rhythmic females (~65%) than males (~16%) (Fig. 1J). The free-running period of the experimental flies was significantly shorter for both sexes (Table 3), as reported previously for males. Rhythmic power was significantly lower than that of the controls for both han^{5304} males and females (Fig. 1K), but the effect was more pronounced in males, suggesting that females have more consolidated rhythms (Fig. 1L). Similar to the effect of the *Pdf* mutation, han^{5304} flies showed significantly higher levels of LD sleep than controls, and this effect was also more pronounced in females (Fig. 1M□O). Taken together, these results suggest that female circadian rhythms are less affected by the loss of both *Pdf* and *PdfR*. However, the LD sleep phenotypes were more pronounced in females.

CRISPR-Cas9-mediated *Pdf* mutagenesis has more pronounced effects on male behavior.

In the *Pdf* null mutant, background effects could contribute to the sexual dimorphism observed in behavioral rhythms. We therefore employed a tissue-specific CRISPR-Cas9-mediated knockout of *Pdf* in both males and females, as described in a recent study that focused on males [50]. To assess the efficiency of the manipulation, we stained for PDF in flies that

constitutively expressed *Pdf* gRNA and Cas9 in *Pdf*+ neurons. This experiment was conducted at 28°C, as this temperature was more effective at mimicking the behavioral phenotypes of the Pdf^{01} mutant males and allows direct comparison with adult-specific manipulation, which requires switching from 18°C to 28°C.

PDF was reduced in the s-LN_vs in both sexes (Fig. 2 A-C), although in most experimental brains, we noted faint staining in the dorsal projections of at least one s-LN_v in at least one brain hemisphere (Fig. 2A). We quantified PDF intensity in the cell bodies of the sLNvs and found that the signal intensity was reduced in both sexes in a similar manner (Fig. 2B-D). PDF expression within the large LN_vs was less affected and could be detected in 2–3 l-LNv cell bodies in most brains (Fig. 2A). In addition to behavioral phenotypes, Pdf^{01} mutation leads to pronounced misrouting of s-LN_v projections in male flies [51] . We employed a transgene expressing a red fluorescent protein under the *Pdf* regulatory sequence [52] and observed faint projections occasionally defasciculating from the main bundle in one or both hemispheres in *Pdf* >*Pdf*-g; *Cas9* flies of both sexes (Fig. 2A, middle panels).

We analyzed activity□rest rhythms in *Pdf* >*Pdf*-g; *Cas9* flies and found that while experimental males were largely arrhythmic, a greater proportion of experimental females remained rhythmic (Fig. 3A-B). The free-running period of the experimental males was not significantly different from that of the controls, but a wide range of periods were observed. Compared with parental controls, *Pdf* >*Pdf*-g; *Cas9* females had significantly shorter free-running periods (Fig. 3C). The rhythmic power was significantly lower in experimental flies of both sexes (Fig. 3D), but the effect was less pronounced in females (Fig. 3E). Sleep under LD was not affected (Fig. S2 A-B), whereas sleep under DD was similarly increased in males and females (Fig. S2 C-E).

We next restricted the CRISPR mutagenesis of *Pdf* to the small LN_vs via a specific driver from the split-Gal4 collection generated by the Rubin Laboratory (*SS00681*-Gal4). *Pdf* knockdown in the s-LNv resulted in most males being arrhythmic (~30% rhythmicity), whereas the experimental females were ~45% rhythmic (Fig. S3A). The percentage of rhythmic flies was significantly lower than that of both controls for experimental males but not for females (Fig.

S3A). The free-running period of the experimental males was shorter than that of their respective control flies, whereas the experimental females did not differ from their controls (Fig. S3B). The rhythmic power of the males was lower than that of the controls, but was not different between the experimental females and their controls (Fig. S3C). This suggests that PDF from the s-LNv is important for the behavioral and sex-specific differences observed in *Pdf*^{01} mutants.

We next conducted adult-specific CRISPR-Cas9 knockdown of *Pdf* (Fig S4). Although a previous study in males did not establish a connection between developmental misrouting caused by *Pdf* downregulation and the disruption of behavioral rhythms in adulthood [51], sex-specific differences observed upon *Pdf* loss may result from developmental effects. The AGES system was previously employed to rule out the developmental effects of the loss of *Pdf* [50], but a recent study showed that AUXIN exposure induces short- and long-term changes in physiology and behavior [53]. Therefore, we employed a temperature-sensitive Gal80 variant with ubiquitous expression to conditionally inhibit Gal4-mediated expression of the *Pdf* guide and Cas9 [54]. This allows for the temporal control of UAS transgenes since Gal80^{ts} is active at lower temperatures but inactive at higher temperatures. We raised the flies at 18°C and transferred them to 28°C immediately after eclosion so that *Pdf* knockout occurred only in adult flies. Consistent with what was reported for males by Gorostiza et al. [51] via RNA-mediated interference (RNAi) of *Pdf*, we did not observe misrouting in experimental flies (Fig. S4A). While PDF levels were significantly reduced in both males and females, the manipulation was substantially more effective in males (Fig S4B-C). Therefore, although the circadian behavioral phenotypes were again more pronounced in males than in females (Fig S4D-F), this is likely due to higher remaining PDF expression in experimental females.

Speeding up the M-cell clock leads to a coherent period shortening only in males.

Next, we sought to determine if the influence of the *Pdf*-releasing cells themselves was sexually dimorphic. While PDF is released from both large and small LN_vs, only s-LN_vs (Morning cells) play key roles in regulating free-running rhythm properties [16]. In males, manipulations that change the pace of the clock specifically in the LN_vs result in changes in the phase of the morning peak of activity and in the free-running period [20, 55]. We expressed the

Doubletime 'short' (*DBT*^{s}) allele [56] under the *Pdf-Gal4* driver (Fig. 4A) and analyzed the effects on behavior in both sexes. We found that *Pdf* > *DBT*^{s} males, but not females, have an advanced phase of the morning peak of activity (M-peak, Fig. 4B-C). This suggests that under LD cycles, the M-oscillator is more effective at setting the phase of male than female behavior.

Under free-running conditions, both *Pdf* > *DBT*^{s} male and female flies showed a significantly lower percentage of rhythmic flies than their controls (Fig. 4D), but there were fewer rhythmic females (~40%) than males (~65%) (Fig. 4D-E). The free-running period of most *Pdf* > *DBT*^{s} males was ~18.5 hours (Fig. 4F), whereas the *Pdf* > *DBT*^{s} females showed a large proportion of individuals with a period of ~24 hours, reflecting the pace of the molecular clock in the rest of the clock network (Fig. 4F). Some *Pdf* > *DBT*^{s} males (~23%) and a smaller proportion of females (~6%) also presented complex rhythms (Table 4). The average period value of the second period component (which has a lower power value) was ~24.07 ± 0.4 for the experimental males and 19.7 ± 0.4 for the experimental females. Neither male nor female control flies exhibited complex rhythms (Table 4). Among rhythmic flies, both *Pdf* > *DBT*^{s} males and females had lower rhythmic power than the controls (Fig. 4G), with no difference between the sexes (Fig. 4H). As a control, we expressed *DBT*^{s} via *Clk856-Gal4* which is expressed in most clock neurons (Fig. S5A). Speeding up the molecular clock in most clock neurons significantly advanced both the morning and evening activity peaks of both males and females (Fig. S5B-D). There were no significant differences between experimental males and females in the percentage of rhythmic flies, rhythmic power, or shortening of free-running periods following DBT expression in all clock neurons (Fig. S5E-G).

These results support the notion that M-cells are more dominant in the male than in the female circadian network. Previous studies have shown that blocking synaptic neurotransmission by expressing the tetanus toxin light chain (TeTxLC) in small and large LN_vs affects male activity rhythms, likely in a *Pdf*-independent manner [57-59]. We analyzed male and female *Pdf* > TeTxLC flies and found that neither sex significantly changed the ability to maintain rhythmicity under free-running conditions (Fig S6A-B). Both sexes significantly lengthened the free-running period, but the effect was more pronounced in males (Fig. S6C-D). Rhythmic power was not affected in experimental flies of either sex (Fig. S6E).

We next asked whether changing the pace of the clock in LNds (E-cells) via *DBT*^{S} expression also had sexually dimorphic effects on behavior. These cells can be subdivided into at least 3 different clusters on the basis of their anatomy [8], physiology [55], transcriptomic profiles [13] and connectivity patterns [15]. The PDFR-expressing E1 and E2 clusters have been shown to regulate evening activity under LD [60, 61] and to be able to maintain free-running activity rhythms in the absence of a functional clock in M cells [62, 63], whereas the behavioral role of the E3 cluster remains unknown. We used the MB122-B split-gal4 driver to target the E1 and E2 subsets (Fig. 5A) and found that while expressing *DBT*^{S} in this group of evening cells significantly advanced the phase of the E-peak in experimental flies of both sexes (Fig. 5B-C), the effect was more pronounced in females (Fig. 5D). Speeding up of clocks in the E1 + E2 LN_ds did not significantly alter the free-running period or rhythmic power of experimental flies of either sex (Fig. 5E-F). M-cells have been shown to be the dominant oscillators in DD and to regulate rhythm properties such as persistence and the free-running period of endogenous locomotor rhythms to a large extent [16, 20, 21, 55], although manipulations of other clock cells can affect rhythm properties to some extent [55, 64]. Thus, speeding up the clock in the PDFR$^+$ E1 and E2 clusters leads to similar behavioral phenotypes in males and females under free-running conditions. Taken together, these results indicate that the relative influence of the M and E subsets of clock neurons are sexually dimorphic.

Discussion

The critical importance of considering sex as a biological variable has gained increasing recognition in biomedical research [65, 66]. Bias toward male subjects is particularly prevalent in neuroscience, with single-sex studies using male animals outnumbering those using female animals at a ratio of 5.5:1 [67]. This disparity extends to chronobiology, resulting in a limited understanding of how sex affects circadian organization in the nervous system. However, work from several laboratories has revealed sexual dimorphism within the SCN and in its input and output pathways [1, 68]. Sex differences in SCN morphology have been described in both animal models and humans, and sex differences in SCN electrical activity and steroid hormone receptors have also been reported (reviewed in [2]). Notably, sex differences in the number of SCN

neurons that express the neuropeptide vasoactive intestinal polypeptide (VIP) and in *Vip* mRNA *e*xpression have been reported (reviewed in [2]). The roles of the mammalian VIP and the *Drosophila* PDF in circadian physiology are highly similar, although neither these peptides nor their receptors are sequence orthologs [69].

Several studies have shown the importance of PDF in generating coherent rhythms of ~24-hour periodicity. Here, we report that females lacking *Pdf* or its receptor *PdfR* are more likely to maintain consolidated activity-rest behavior than males. This could be because of sex differences in PDF signaling mechanisms, PDFR expression, or the influence of other clock neurons within the network. We did not detect sex differences in the overall levels or temporal patterns of PDF accumulation, suggesting that these differences might not contribute to the sexually dimorphic effects of the loss of *Pdf* expression. In males, other neuropeptides are known to act in concert with PDF to maintain consolidated rhythms in the network, although none of them have as profound an effect as PDF in regulating activity-rest rhythms in DD [46, 70]. Single mutants of DH31 and CCHamide1 do not affect activity rhythms by themselves, but the double mutants of these neuropeptides along with Pdf^{01} ($DH31^{01}/Pdf^{01}$ and $Pdf^{01}/CCHa^{SK8}$) are almost completely arrhythmic, suggesting that these neuropeptides act hierarchically in the network, with PDF being at the top of that hierarchy [46, 70]. The importance of PDF relative to other peptides released by clock neurons may also be sexually dimorphic.

To overcome the possible pleiotropic effects of Pdf^{01} and *PdfR* mutations, we employed a constitutive knockout of *Pdf* in ventral lateral neurons via the CRISPR-Cas9 method. Although CRISPR manipulation was only partially effective at eliminating PDF expression, it nevertheless produced phenotypes reminiscent of those produced by the Pdf^{01} mutation. We observed faint staining in the dorsal projections of at least one s-LN_v in at least one hemisphere in most brains, and PDF staining in a single s-LN_v projection reaching the dorsal brain has been shown to be sufficient for behavioral rhythms [71]. Experimental flies in which *Pdf* was knocked out starting at the onset of promoter expression early in development showed extensive misrouting of their dorsal termini, similar to what has been reported for Pdf^{01} males [51]. Instances of s-LN_v misrouting have also been observed in other core clock mutants, such as per^{01} and tim^{01} [72] and cyc^{01} [73]. We observed misrouting in experimental flies of both sexes (data not shown), and no

correlation between misrouting and behavioral phenotypes was found by others for *Pdf*^{01} males [51]. Importantly, *Pdf* > *Pdfg;Cas9* manipulation recapitulates the sexually dimorphic circadian phenotypes of *Pdf*^{01} mutants: a larger fraction of females are rhythmic, and females exhibit greater rhythm power.

In males, changing the speed of the M cell clock leads to phase changes in the morning peak under LD [60]. To determine whether M-cell manipulations also have sexually dimorphic effects on behavior, we sped up the molecular clock by expressing the *Doubletime short* allele (*DBT*$^{s)}$. Surprisingly, our results revealed that speeding up the clock of M-cells advances the phase of the morning peak in males, whereas the female morning peak phase is not affected. These results support previous studies conducted in males on the role of M-cells in regulating the morning peak of activity [16, 21, 60] and suggest that M-cells are unable to regulate the phase of morning activity in the same way in females. In DD, males had largely coherent short-term rhythms, and the majority (65%) were rhythmic. In contrast, only 40% of the females were rhythmic, and their period showed a bimodal distribution, with most flies exhibiting an ~24-hour period. These findings further support the notion that M-cells are less dominant than the circadian clock network in females. A possible explanation for this is that other clock neurons are able to “resist” their influence, and the conflict between the fast-paced M cell clock and the ~24 clock other clock neurons is what leads to greater arrhythmicity in females.

The expression of a tetanus toxin light chain construct in flies blocks neurotransmission by binding and cleaving the synaptic protein Synaptobrevin [74]. Expressing tetanus toxin in ventral lateral neurons does not affect behavioral rhythmicity and lengthens the free-running period in males, as reported in previous studies [58, 59, 75]. The behavioral phenotypes resulting from the blockade of synaptic transmission differ from those resulting from the loss of PDF [18] or the ablation of *Pdf*-expressing neurons [21], possibly because tetanus toxin affects classical transmission and not the dense core vesicle-mediated release of neuropeptides such as PDF [76]. Abrogating the dorsal termini of the small ventral lateral neurons, where most of the output synapses are found [15, 76], does not result in behavioral phenotypes similar to those of *Pdf*^{01} under either LD or DD [22]. Our results show that blocking synaptobrevin-dependent synaptic transmission in M-cells does not affect rhythmicity but rather lengthens the free-running period.

The period lengthening is more pronounced in males, supporting the notion that M-cells have a greater influence on the circadian network in males.

Cryptochrome and *PdfR*-expressing clusters of evening cells—the sNPF-expressing E1 cluster and the ITP-expressing E2 cluster [77]—have roles in setting the phase of the E-peak under LD and sustaining behavioral rhythms in the absence of a functional molecular clock in M-cells [62, 63]. To test whether these cells have a differential influence on the network in males and females, we expressed DBT^S under a driver that is expressed specifically in the E1 and E2 subsets of LN_ds. Our results showed that speeding up the clocks in the E1+E2 clusters resulted in a phase advance in the evening peak of activity in both sexes, but the effect was more pronounced in females. Neither MB122 > DBT^S males nor females presented phenotypes under free-running conditions. A possible reason for the behavioral differences observed between the sexes could be redundancy in females, such that the network is not as dependent on PDF or M-cells for timekeeping. This finding suggests that the female network could have a more distributed mode of timekeeping throughout the circadian clock network.

Across species, sex differences in the circadian timing system are largely related to the regulation of reproduction-related behaviors. In mammals, the SCN determines the timing of the release of reproductive hormones and influences the timing of mating (reviewed in [68]) and aggression [78]. In *Drosophila*, the circadian clock controls the timing of sex-specific and sexually dimorphic behaviors, such as male courtship [79] and female sexual receptivity [80] and egg laying [81]. This regulation of rhythmic behaviors requires connectivity between clock neurons and downstream sex-specific circuits. For example, the $DN1_p$ cluster, which has been shown to be more active in males [36], is functionally connected to the male-specific *fru*-expressing P1 neurons that regulate male courtship [37]. In females, Allostatin C-producing $DN1_p$s have been shown to connect to downstream targets to control rhythms in oogenesis [82], and the Janelia female hemibrain connectome revealed that the LN_ds form connections with the *doublesex*-expressing PC1 cluster [15]. Our data suggest that the relative hierarchy of circadian oscillators is sexually dimorphic, with a less dominant M oscillator in females. This pattern of circadian timekeeping may serve an adaptive purpose, ensuring the precise timing of essential

female-specific behaviors crucial for reproductive fitness, such as sexual receptivity and egg laying.

Acknowledgments

We are grateful to Charlotte Helfrich-Forster, Abhilash Lakshman, Cahir O'Kane, Jeff Price, and Paul Taghert for helpful discussions and Orie Shafer and members of the Fernandez Lab for helpful comments on the manuscript. We also thank Justin Blau, Aljoscha Nern, Gerry Rubin, Michael Rosbash, and Paul Taghert for sharing fly lines. The mouse anti-PDF antibody was obtained from the Developmental Studies Hybridoma Bank, created by the NICHD of the NIH and maintained at The University of Iowa, Department of Biology, Iowa City, IA 52242. Stocks obtained from the Bloomington *Drosophila* Stock Center (NIH P40OD018537) were used in this study. This work was supported by an NIH grant (R01NS118012) and an NSF Grant (IOS-2239994) to M.P.F. and a Beckman Foundation Scholarship to E.S-C.

Materials and methods

Fly lines and rearing.

All the genotypes were reared on corn syrup soy media (Archon Scientific; Durham, NC) under LD 12:12 cycles at 25°C unless specified otherwise (see figure legends for details). The fly lines used in this study were *Canton-S*, w^{1118}, Pdf^{01}, $PdfR^{01}$, *Pdf-RFP*, *Pdf-Gal4; tub-Gal80*^{ts}, UAS-*Cas9;* UAS-*Pdfg*, *Pdf-Gal4*, UAS-*DBT*^{s}, *UAS TeTxLC*, *Clk856Gal4*, *s-LNvGal4*, and *MB122B-Gal4*. See the fly lines and reagents table below for more details.

Activity□rest behavior recording and analysis.

Individual male and virgin female flies (3–5 days old) were housed in glass locomotor tubes containing 2% agar□4% sucrose food on one end and yarn on the other end. Locomotor activity was recorded using Drosophila activity monitors (DAM, Trikinetics, Waltham, United States of America). The experiments were conducted in Tritech or Percival incubators under controlled light and temperature conditions. Flies were entrained to 12:12 LD cycles for at least 5 days and then transferred to constant darkness (DD) for at least 7 days at a constant temperature of 25°C unless otherwise specified (see figure legends for details). The raw data obtained from the DAM system were scanned and binned into activity counts of 15 min intervals via the DAM File scan. The data were analyzed via the CLOCKLAB software (Actimetrics, Wilmette, IL).

The values of period and rhythmic power were calculated for a period of 7 days via a chi-square periodogram with a cutoff of $p = 0.01$. The rhythmic power for each designated rhythmic fly was determined by subtracting the chi-square significance value from the power of the periodogram. Flies that did not exhibit a periodicity peak above the significance threshold were categorized as "arrhythmic," and their period and rhythmic power were not included in the analysis. The values of the morning and evening peaks were calculated via PHASE software [83]. The total LD sleep values for all the genotypes were calculated for a period of 3 days (LD days 2--4) via the PHASE software. Representative actograms were generated via ClockLab, and activity plots were generated via PHASE. The period, rhythmic power, total sleep, and phase values of all the flies for a particular experimental genotype were compared against the background or parental controls via either the Mann□Whitney test or the Kruskal□Wallis

ANOVA followed by the Dunn's multiple comparisons test. The details of the statistical comparisons and the number of flies used in a given experiment are indicated in their respective figure legends. The number of rhythmic flies of the experimental genotype was compared against their respective background or parental controls via Fisher's exact test. All the statistical analyses were performed via GraphPad Prism 9.0.

Immunohistochemistry

The brains of adult male or female flies were dissected in ice-cold Schneider's insect media (S2) and fixed immediately after dissection in 2% paraformaldehyde (PFA) in S2 media for 30 minutes at room temperature. The fixed brains were washed (three washes of 10 minutes each) with 0.3% PBS-Triton X 100 (PBS-TX) and then treated with blocking solution (5% normal goat serum made in 0.3% PBS-TX) for 1 hr at room temperature. The brains were then incubated with primary antibodies at 4°C for 24 hrs. The primary antibodies used were anti-PDF (mouse, 1:3000, C7, DSHB) and anti-RFP (rabbit, 1:2000, Rockland Immunochemicals). After incubation, the brains were subjected to six washes with 0.3% PBS-TX and incubated with Alexa Fluor-conjugated secondary antibodies overnight at 4°C. The following secondary antibodies were used: goat anti-mouse 488 (1:3000, Invitrogen) and goat anti-rabbit 568 (1:3000, Invitrogen). After incubation, the brain samples were washed 6 times with 0.3% PBS-TX, cleaned and mounted on a clean glass slide using Vectashield mounting media.

Image acquisition and analysis

The brains were imaged via a confocal microscope (Olympus FV3000) with an Olympus UPLanXApo 20x or 40x objective. Image analysis was performed via Fiji software [84]. In the samples, small and large ventral lateral neurons were classified on the basis of their anatomical locations and expression of the PDF. PDF intensities in these cells were measured by selecting the slice of the Z-stack that showed the maximum intensity, drawing a region of interest (ROI) around the cells and measuring their intensities. Three to four separate background values were also measured around each cell, and the final intensity was taken as the difference between the cell intensity and the average background.

For quantification of the PDF in the dorsal projections, a rectangular box was drawn as the ROI starting from the point where the PDF projection turns into the dorsal brain and the intensity is measured. Three to four background values were also measured around the projection. The intensity values obtained from both hemispheres for each cell type for each brain were averaged and used for statistical analysis. PDF intensity from the s-LN_v was compared between the experimental and control genotypes via a Mann Whitney test. To estimate different aspects of rhythmicity in PDF oscillations in the dorsal termini of s-LN_v in males and females, we used a COSINOR-based curve-fitting method (Cornelissen, 2014). COSINOR analysis was implemented via the CATCosinor function from the CATkit package written for R [85].

Fly lines and reagents.

REAGENT or RESOURCE	SOURCE	IDENTIFIER
Experimental Models: Organisms/Strains		
Canton-S	Bloomington *Drosophila* Stock Center	BDSC 64349
w^{1118};+;+	Bloomington *Drosophila* Stock Center	BDSC 3605
yw;Pdf-RFP,Pdf-Gal4;Tub-gal80^{ts}	Justin. Blau, NYU	
w;;Pdf^{01}	Paul Taghert, Wash U Med. School	
w PdfR^{01}*;;*	Paul Taghert, Wash U Med. School	
w; Pdf-gal4; +	Paul Taghert, Wash U Med. School	
;UAS Cas9; pdfg	Michael Rosbash, Brandeis University	BDSC 99650
w;+;DBT^{s}	Jeffrey Price, University of Missouri	

w; MB122B-Gal4; +	Gerry Rubin, HHMI Janelia Research Campus	
w; Clk856-Gal4; +	Orie Shafer, CUNY ASRC	
s-LNv Gal4	Gerry Rubin, Janelia Research Campus	SS00681-Gal4
w; UAS TeTxLC; +	Cahir O'Kane, University of Cambridge	
Antibodies		
Rabbi anti-RFP (1:2000)	Rockland	#600-401-379-RTU
Mouse anti-PDF (1:3000)	Developmental Studies Hybridoma Bank	
Anti-rabbit Alexa-568 (1:3000)	Thermo Fisher	A11036
Anti-mouse Alexa-488 (1:3000)	Thermo Fisher	A11029
Software		
Fiji	http://fiji.sc	RRID: SCR_002285
MATLAB R2022b	MathWorks, Natick	RRID: SCR_001622
GraphPad Prism 9.0	GraphPad Software	RRID: SCR_002798
DAM FileScan	Trikinetics	
ClockLab	Actimetrics	RRID:SCR_014309
Chemicals, Peptides, and Recombinant Proteins		
Vectashield Mounting Medium	Vector Laboratories	#H-1000-10
Premix PBS Buffer (10x)	Sigma□Aldrich	Cat# 11666789001
2% Paraformaldehyde (PFA)	Sigma□Aldrich	47608-250ML-F

Triton- X-100	Bio Basic	CAS#9002-93-1
Schneider's *Drosophila* Medium (S2)	Thermo Fisher	21720024
Other		
DAM2 *Drosophila* Activity Monitors	Trikinetics	
DAM Drosophila Environmental Monitors	Trikinetics	

Figure legends.

Figure 1: Mutations in *Pdf* and *PdfR* lead to sexually dimorphic phenotypes. (A) Representative double-plotted actograms of w^{1118} (left) and Pdf^{01} (right) male flies subjected to 6 days of LD followed by seven days of DD. **(B)** Representative actograms of w^{1118} (left) and Pdf^{01} (right) female flies subjected to six days of LD followed by seven days of DD. **(C)** Percentages of rhythmic flies are plotted for control (w^{1118}) and Pdf^{01} males (left, n = 86 (w^{1118}), n = 81 (Pdf^{01})) and females (right, n = 75 (w^{1118}), n = 101 (Pdf^{01})). The error bars represent the SEM values plotted across three replicate experiments. **(D)** Rhythmic power of control (w^{1118}) and Pdf^{01} male and females was calculated via a Chi-square Periodogram. **(E)** The differences in rhythmic power between experimental males and females and their respective controls are plotted. **(F)** Average sleep plots of flies over seven days in DD are plotted for male and female control (w^{1118}) and experimental (Pdf^{01}) flies. **(G)** Average sleep plots under LD 12:12 for the control (w^{1118}) and experimental (Pdf^{01}) groups are plotted for males (left) and females (right). The plots are averaged over flies and days for a period of three days under LD 12:12. **(H)** Total sleep values under LD conditions are plotted for male (left) and female (right) control (w^{1118}) and experimental (Pdf^{01}) flies. **(I)** The differences in total LD sleep values between experimental males and females and their respective controls are plotted. **(J)** Percentages of rhythmic flies are plotted for the control (w^{1118}) and han^{5304} males (left, n = 86 (w^{1118}), n = 115 (han^{5304})) and females (right, n = 74 (w^{1118}), n = 94 (han^{5304})) **(K).** Rhythmic power of the control (w^{1118}) and

han^{5304} males and females calculated via the chi-square periodogram are plotted. **(L)** The differences in rhythmic power between experimental males and females and their respective controls are plotted. **(M)** Average sleep plots under LD 12:12 for control (*w*^{1118}) and experimental (*han*^{5304}) flies are plotted for males (left) and females (right). The plots are averaged over flies and days for a period of three days under LD 12:12. **(N)** Total sleep values under LD conditions are plotted for male (left) and female (right) control (*w*^{1118}) and experimental (*han*^{5304}) flies. **(O)** The differences in total LD sleep values between experimental males and females and their respective controls are plotted. Statistical comparisons were performed between the control and experimental flies of both sexes using a Mann□Whitney U test. The box plots extend from the 25th to 75th percentile, with whiskers extending from the smallest to the largest value, and each point represents data from a single fly. Combined data from at least three replicate experiments are plotted. * $p < 0.05$, ** $p < 0.01$, *** $p < 0.001$.

Figure 2: Tissue-specific CRISPR-mediated *Pdf* manipulation leads to a reduction in PDF levels and the misrouting of s-LN$_v$ dorsal termini in both sexes. (A) Representative confocal images of control (*Pdf-RFP, Pdf-Gal4; tub-Gal80*^{ts}) (top) and experimental (*Pdf-RFP, Pdf-Gal4; tub-Gal80*^{ts} *> Cas9; Pdf-g*) (middle, males; bottom, females) flies stained with RFP and PDF antibodies. Experimental flies show a significant reduction in PDF levels in the sLN$_v$s (white arrows, PDF channel) and misrouting of the s-LN$_v$ dorsal termini (white arrows, RFP channel). **(B)** Representative confocal images of the small and large LN$_v$s of control (*Pdf-RFP, Pdf-Gal4; tub-Gal80*^{ts}) (top) and experimental (*Pdf-RFP, Pdf-Gal4; tub-Gal80*^{ts} *> Cas9; Pdf-g*) (bottom) brains stained with RFP and PDF antibodies. **(C)** Quantification of PDF levels from s-LN$_v$ cell bodies in control (*Pdf-RFP, Pdf-Gal4; tub-Gal80*^{ts}) and experimental (*Pdf-RFP, Pdf-Gal4; tub-Gal80*^{ts} *> Cas9; Pdf-g*) flies are plotted for males (left) and females (right). $n > 12$ brains for all genotypes. **(C)** Differences in the PDF intensity values of experimental males and females from their respective parental controls. Statistical comparisons were performed between the control and experimental flies of both sexes using the Mann□Whitney U test. The box plots extend from the 25th to 75th percentile, with whiskers extending from the smallest to the largest value, and each point represents data from a single fly. Combined data from at least two replicate experiments are plotted. * $p < 0.05$, ** $p < 0.01$, *** $p < 0.001$. Scale bars = 50 μm.

Figure 3: CRISPR-Cas9-mediated *Pdf* mutagenesis has more pronounced effects on male behavior. (A) Representative actograms of control (*Pdf-RFP, Pdf-Gal4; tub-Gal80^{ts}*) and *(UAS Cas9; Pdf-g)* and experimental (*Pdf-RFP, Pdf-Gal4; tub-Gal80^{ts} > Cas9; Pdf-g*) males (left) and females (right) are plotted for six days of LD followed by nine days of DD. **(B)** Percentages of rhythmic flies are plotted for control (*Pdf-RFP, Pdf-Gal4; tub-Gal80^{ts}) and (UAS Cas9; Pdf-g)* and experimental (*Pdf-RFP, Pdf-Gal4; tub-Gal80^{ts} > Cas9; Pdf-g)* males (left, *n* = 85 (*Pdf-RFP, Pdf-Gal4; tub-Gal80^{ts}*), *n* = 89 (*UAS Cas9; Pdf-g*), *n* = 106 (*Pdf-RFP, Pdf-Gal4; tub-Gal80^{ts} > Cas9; Pdf-g*) and females (right, *n* = 79 (*Pdf-RFP, Pdf-Gal4; tub-Gal80^{ts}*), *n* = 78 (*UAS Cas9; Pdf-g*), *n* = 85 (*Pdf-RFP, Pdf-Gal4; tub-Gal80^{ts} > Cas9; Pdf-g).* The error bars represent SEM values plotted across three replicate experiments. **(C)** Free-running periods of control (*Pdf-RFP, Pdf-Gal4; tub-Gal80^{ts} and UAS Cas9; Pdf-g)* and experimental (*Pdf-RFP, Pdf-Gal4; tub-Gal80^{ts} > Cas9; Pdf-g)* males (left) and females (right) calculated via the chi-square periodogram are plotted. **(D)** Rhythmic power of control (*Pdf-RFP, Pdf-Gal4; tub-Gal80^{ts} and UAS Cas9; Pdf-g)* and experimental (*Pdf-RFP, Pdf-Gal4; tub-Gal80^{ts} > Cas9; Pdf-g)* males (left) and females (right) calculated via the chi-square periodogram are plotted. **(E)** The differences in rhythmic power of experimental males and females from their respective controls are plotted. Flies were kept at 28°C throughout development, and as adults, experiments were conducted at 28°C. Statistical comparisons were performed between the control and experimental flies of both sexes using the Kruskal Wallis test followed by Dunn's multiple comparisons test for panels 3B-3D and Mann-Whitney U test for Fig. 3E. The box plots extend from the 25th to 75th percentile, with whiskers extending from the smallest to the largest value, and each point represents data from a single fly. Combined data from at least three replicate experiments are plotted. ** $p < 0.01$, *** $p < 0.001$.

Figure 4: Speeding up the clock in M-cells leads to sexually dimorphic phenotypes. (A) Depiction of the adult *Drosophila* brain hemisphere indicating the clock cell subsets (colored) having a faster running molecular clock. **(B)** Average activity plots of control (*Pdf-Gal4*) and (UAS-*DBT^{s}*) and experimental (*Pdf > DBT^{s}*) flies are plotted for males (left) and females (right). The plots are averaged over flies and days for a period of three days under LD 12:12. **(C)** The

phase of the morning peak of activity under LD 12:12 is plotted for control (*Pdf-Gal4*), (UAS-*DBT*^{s}) and experimental (*Pdf >DBT*^{s}) males (left, *n* = 116 (*Pdf-Gal4*), *n* = 120 (UAS-*DBT*^{s}), *n* = 88 (*Pdf > DBT*^{s})) and females (right, *n* = 85 (*Pdf-Gal4*), *n* = 109 (UAS-*DBT*^{s}), *n* = 73 (*Pdf > DBT*^{s})). **(D)** Percentages of rhythmic flies are plotted for controls (*Pdf-Gal4), (UAS-DBT*^{s}*),* and experimental (*Pdf > DBT*^{s}*)* males (left, *n* = 90 (*Pdf-Gal4*), *n* = 108 (*UAS-DBT*^{s}), *n* = 93 (*Pdf > DBT*^{s}) and females (right, *n* = 66 (*Pdf-Gal4*), *n* = 83 (*UAS-DBT*^{s}), *n* = 70 (*Pdf > DBT*^{s}*).* The error bars represent the SEM values plotted across three replicate experiments. **(E)** Representative actograms of control (UAS-*DBT*^{s}) and experimental (*Pdf > DBT*^{s}) males (left) and females (right) plotted for six days of LD followed by ten days of DD. **(F)** Free-running periods of control (*Pdf-Gal4), (UAS-DBT*^{s}*)* and experimental (*Pdf > DBT*^{s}*)* males (left) and females (right) calculated via the chi-square periodogram are plotted. **(G)** Rhythmic power of control (*Pdf-Gal4), (UAS-DBT*^{s}*)* and experimental (*Pdf > DBT*^{s}*)* males (left) and females (right) calculated via the chi-square periodogram are plotted. **(H)** The differences in rhythmic power between experimental males and females and their respective controls are plotted. Statistical comparisons were performed between the control and experimental flies of both sexes using the Kruskal□Wallis test followed by Dunn's multiple comparisons test for panels 4C, 4F, and 4G and Mann-Whitney U test for Fig. 4H. The box plots extend from the 25th to 75th percentile, with whiskers extending from the smallest to the largest value, and each point represents data from a single fly. Combined data from at least three replicate experiments are plotted. * $p < 0.05$, ** $p < 0.01$, *** $p < 0.001$.

Figure 5: Speeding up the clock in an E-cell subset leads to a more advanced evening peak in females. (A) Depiction of the adult *Drosophila* brain hemisphere indicating the clock cell subsets (colored) having a faster running molecular clock. **(B)** Average activity plots of control (*MB122B-Gal4*) and (*UAS-DBT*^{s}) and experimental (*MB122B > DBT*^{s}) flies are plotted for males (left) and females (right). The plots are averaged over flies and days for a period of three days under LD 12:12. **(C)** Phase of the evening peak of activity under LD 12:12 for controls (*MB122B-Gal4*) and (*UAS-DBT*^{s}) and experimental (*MB122B > DBT*^{s}) males (left, *n* = 92 (*MB122B-Gal4*), *n* = 93 (*UAS-DBT*^{s}), *n* = 93 (*MB122B > DBT*^{s})) and females (right, *n* = 85 (*MB122B-Gal4*), *n* = 87 (*UAS-DBT*^{s}), *n* = 89 (*MB122B > DBT*^{s})). **(D)** The differences in the

phase of the E peak between experimental males and females and their respective controls are plotted. **(E)** Free-running period of control (*MB122B-Gal4* and *UAS-DBT^{s})* and experimental (*MB122B > DBT^{s})* males (left) and females (right) calculated via the chi-square periodogram are plotted. **(F)** Rhythmic power of control (*MB122B-Gal4 and UAS-DBT^{s})* and experimental (*MB122B > DBT^{s})* males (left) and females (right) calculated via the chi-square periodogram are plotted. Statistical comparisons were performed between the control and experimental flies of both sexes using the Kruskal Wallis test followed by Dunn's multiple comparisons test for panels 5C, 5E, and 5F and Mann-Whitney U test for Fig. 5D. The box plots extend from the 25th to 75th percentile, with whiskers extending from the smallest to the largest value, and each point represents data from a single fly. Combined data from at least three replicate experiments are plotted. ** $p < 0.01$, *** $p < 0.001$.

Supplementary figures

Figure S1: PDF rhythmic accumulation is similar in males and females (related to Figure 1.)

(A) Representative confocal images of control (*w^{1118}*) (top) and experimental (*Pdf^{01}*) (bottom) male and female flies stained with the PDF antibody. **(B)** Scatterplots of PDF staining intensities of the s-LN$_v$ dorsal projections of both male and female flies plotted at different time points over a 24-hr cycle on DD day 3. Each dot represents the mean PDF intensity value averaged over both hemispheres of one brain. The cyan and pink lines are the best fit cosine curves from the parameters that were extracted via COSINOR analysis. See Table 2 for more details. **(C)** Amplitude values of PDF oscillation obtained from COSINOR curve fits are plotted for male and female flies. The error bars are 95% CI values calculated from the standard error obtained from COSINOR analysis. The overlapping error bars indicate that the amplitude values of males and females are not significantly different. n > 7 brain samples/time point.

Figure S2: CRISPR-Cas9-mediated *Pdf* mutagenesis has similar effects on male and female sleep. (Related to Figure 3.) (A) Average sleep plots under LD 12:12 of control (*Pdf-RFP, Pdf-Gal4; tub-Gal80^{ts} and UAS Cas9; Pdf-g)* and experimental (*Pdf-RFP, Pdf-Gal4; tub-Gal80^{ts} > Cas9; Pdf-g)* males (left) and females (right) are plotted. The plots are averaged over flies and

days for a period of 3 days under LD 12:12. **(B)** Total sleep values under LD conditions are plotted for control (*Pdf-RFP, Pdf-Gal4; tub-Gal80^{ts} and UAS Cas9; Pdf-g)* and experimental (*Pdf-RFP, Pdf-Gal4; tub-Gal80^{ts} > Cas9; Pdf-g)* males (left) and females (right). **(C)** Average sleep plots of flies over seven days in DD are plotted for male and female control (*Pdf-RFP, Pdf-Gal4; tub-Gal80^{ts} and UAS Cas9; Pdf-g*) and experimental (*Pdf-RFP, Pdf-Gal4; tub-Gal80^{ts} > Cas9; Pdf-g*) flies. **(D)** Total sleep values under DD conditions are plotted for control (*Pdf-RFP, Pdf-Gal4; tub-Gal80^{ts} and UAS Cas9; Pdf-g)* and experimental (*Pdf-RFP, Pdf-Gal4; tub-Gal80^{ts} > Cas9; Pdf-g)* males (left) and females (right). **(E)** The differences in the total DD sleep values of experimental males and females from their respective controls are plotted. Statistical comparisons were performed between the control and experimental flies of both sexes using the Kruskal Wallis test followed by Dunn's multiple comparisons test for panels S2B and S2D and Mann-Whitney U test for Panel S2E. The box plots extend from the 25th to 75th percentile, with whiskers extending from the smallest to the largest value, and each point represents data from a single fly. Combined data from at least three replicate experiments are plotted. ** $p < 0.01$, *** $p < 0.001$.

Figure S3: CRISPR-Cas9-mediated *Pdf* mutagenesis in small ventral lateral neurons has more pronounced effects on male circadian behavior. (A) Percentages of rhythmic flies are plotted for control (*s-LNv-Gal4) and (UAS Cas9; Pdf--g)* and experimental (*s-LNv > Cas9; Pdf--g)* males (left, n = 16 for all genotypes) and females (right, n = 16 for all genotypes). **(B)** Free-running period of control (*s-LNv-Gal4 and UAS Cas9; Pdf-g)* and experimental (*s-LNv > Cas9; Pdf-g)* males (left) and females (right) calculated via the chi-square periodogram are plotted. **(C)** Rhythmic power of control (*s-LNv-Gal4 and UAS Cas9; Pdf-g)* and experimental (*s-LNv > Cas9; Pdf-g)* males (left) and females (right) calculated via the chi-square periodogram are plotted. * $p < 0.05$, ** $p < 0.01$, *** $p < 0.001$. Statistical comparisons were performed between the control and experimental flies of both sexes using the Kruskal Wallis test followed by Dunn's multiple comparisons test. The box plots extend from the 25th to 75th percentile, with whiskers extending from the smallest to the largest value, and each point represents data from a single fly. * $p < 0.05$, ** $p < 0.01$, *** $p < 0.001$.

Figure S4: Adult-specific CRISPR-Cas9-mediated *Pdf* mutagenesis is more effective in males. (Related to Figure 3.) (A) Representative confocal images of control (*Pdf-RFP, Pdf-Gal4; tub-Gal80^{ts}*) (top) and experimental (*Pdf-RFP, Pdf-Gal4; tub-Gal80^{ts} > Cas9; Pdf-g*) male (middle) and female (bottom) flies stained with RFP and PDF antibodies. The experimental flies presented a significant reduction in PDF levels but no misrouting of the s-LN$_v$ dorsal termini. **(B)** Quantification of PDF intensity from s-LN$_v$ cell bodies in control (*Pdf-RFP, Pdf-Gal4; tub-Gal80^{ts}*) and experimental (*Pdf-RFP, Pdf-Gal4; tub-Gal80^{ts} > Cas9; Pdf-g*) flies are plotted for males (left) and females (right). The data points represent the intensity from a single brain sample. n > 10 brains for all genotypes. **(C)** The differences in PDF intensity values of experimental males and females from their respective controls are plotted. **(D)** Percentages of rhythmic flies are plotted for control (*Pdf-RFP, Pdf-Gal4; tub-Gal80^{ts})* and *(UAS Cas9; Pdf-g)* and experimental (*Pdf-RFP, Pdf-Gal4; tub-Gal80^{ts} > Cas9; Pdf-g)* males (left, n = 103 (*Pdf-RFP, Pdf-Gal4; tub-Gal80^{ts}*), n = 109 (*UAS Cas9; Pdf-g*), n = 115 (*Pdf-RFP, Pdf-Gal4; tub-Gal80^{ts} > Cas9; Pdf-g*) and females (right, n = 96 (*Pdf-RFP, Pdf-Gal4; tub-Gal80^{ts}*), n = 90 (*UAS Cas9; Pdf-g*), n = 119 (*Pdf-RFP, Pdf-Gal4; tub-Gal80^{ts} > Cas9; Pdf-g).* **(E)** Free-running periods of control (*Pdf-RFP, Pdf-Gal4; tub-Gal80^{ts} and UAS Cas9; Pdf-g)* and experimental (*Pdf-RFP, Pdf-Gal4; tub-Gal80^{ts} > Cas9; Pdf-g)* males (left) and females (right) calculated via the chi-square periodogram are plotted. **(F)** Rhythmic power of control (*Pdf-RFP, Pdf-Gal4; tub-Gal80^{ts} and UAS Cas9; Pdf-g)* and experimental (*Pdf-RFP, Pdf-Gal4; tub-Gal80^{ts} > Cas9; Pdf-g)* males (left) and females (right) calculated via the chi-square periodogram are plotted. Flies were raised at 18°C until eclosion and were then transferred to 28°C as adults. The flies were kept at 28°C for a period of four to five days before their activity-rest behavior was recorded at 28°C. Statistical comparisons were performed between the control and experimental flies of both sexes using the Kruskal-Wallis test followed by Dunn's multiple comparisons test for panels S4E-F and Mann-Whitney U test for panels S4B-C. The box plots extend from the 25th to 75th percentile, with whiskers extending from the smallest to the largest value, and each point represents data from a single fly. Combined data from at least three replicate experiments are plotted. Scale bars represent 50 μm. * $p < 0.05$, ** $p < 0.01$, *** $p < 0.001$.

Figure S5: Speeding up the clock in all clock cells leads to a phase advance and shortening of the free-running period of activity rhythms (related to Figures 4 and 5). (A) Diagram of

an adult *Drosophila* brain hemisphere indicating the clock cell subsets (blue) expressing DBT$^{s.}$ **(B)** Average activity plots of control (*Clk856-Gal4*) and (UAS-*DBT*^{s}) and experimental (*Clk856 > DBT*^{s}*)* flies are plotted for males (left) and females (right). The plots are averaged over flies and days for a period of three days under LD 12:12. **(C)** Phases of the morning peak of activity under LD 12:12 for controls (*Clk856-Gal4*) and (*UAS-DBT*^{s}) and experimental (*Clk856 > DBT*^{s}) males (left, *n* = 62 (*Clk856-Gal4*), *n* = 57 (*UAS--DBT*^{s}), *n* = 60 (*Clk856 > DBT*^{s})) and females (right, *n* = 59 (*Clk856-Gal4*), *n* = 59 (*UAS--DBT*^{s}), *n* = 50 (*Clk856 > DBT*^{s})) are plotted. **(D)** Phase of the evening peak of activity under LD 12:12 for controls (*Clk856--Gal4*) and (*UAS-DBT*^{s}) and experimental (*Clk856 > DBT*^{s}) males (left) and females (right) are plotted. **(E)** Percentages of rhythmic flies are plotted for control (*Clk856--Gal4*) and (*UAS-DBT*^{s}) and experimental (*Clk856 > DBT*^{s}) males (left) and females (right). The error bars represent the SEM values plotted across two replicate experiments. **(F)** Free-running periods of rhythmic flies calculated via the chi-square period are plotted for controls (*Clk856--Gal4*) and (*UAS-DBT*^{s}) and experimental (*Clk856 > DBT*^{s}) males (left) and females (right). **(G)** Rhythmic power of flies calculated via the chi-square periodogram is plotted for controls (*Clk856--Gal4*) and (*UAS-DBT*^{s}) and experimental (*Clk856 > DBT*^{s}) males (left) and females (right). Statistical comparisons were performed between the control and experimental flies of both sexes via Kruskal□Wallis test followed by Dunn's multiple comparisons test. The box plots extend from the 25th to 75th percentile, with whiskers extending from the smallest to the largest value, and each point represents data from a single fly. Combined data from at least two replicate experiments are plotted. * $p < 0.05$, ** $p < 0.01$, *** $p < 0.001$.

Figure S6: Blocking neurotransmission in *Pdf*-expressing cells leads to more pronounced lengthening of the free-running period in males. (Related to Figure 6). (A) Representative actograms of control *(Pdf-Gal4*), and (*UAS TeTxLC*) and experimental (*Pdf > TeTxLC*) males (left) and females (right) are plotted for five days of LD followed by eight days of DD. **(B)** Percentage of rhythmic flies are plotted for control (*Pdf-Gal4*), and (*UAS TeTxLC*), and experimental (*Pdf > TeTxLC*) males (left, n = 56 (*Pdf-Gal4*), n = 51 (UAS *TeTxLC*), n = 52 (*Pdf > TeTxLC*) and females (right, n = 53 (*Pdf-Gal4*), n = 52 (*UAS TeTxLC*), n = 52 (*Pdf > TeTxLC*). Error bars are SEM values plotted across two replicate experiments. **(C)** Free-running period of control (*Pdf-Gal4* and UAS *TeTxLC*) and experimental (*Pdf > TeTxLC*) males (left) and females

(right) calculated using the Chi-square Periodogram are plotted. **(D)** The difference in free-running period of experimental males and females from their respective controls are plotted. **(E)** Rhythmic power of control (*Pdf-Gal4* and *UAS TeTxLC*) and experimental (*Pdf > TeTxLC*) males (left) and females (right) calculated using the Chi-square periodogram are plotted. Statistical comparisons were performed between the control and experimental flies for both sexes using the Kruskal-Wallis test followed by the Dunn's multiple comparisons test for all panels except S6D where comparisons were made using the Mann Whitney U test. The box plots extend from the 25th to 75th percentile, with whiskers extending from the smallest to the largest value, and each point representing data from a single fly. Combined data from at least two replicate experiments are plotted.

Table 1: Table representing the % rhythmicity, phase of the E peak, free-running period and rhythmic power of w^{1118} and Pdf^{01} males and females.

Pdf^{01}				
Genotype	% Rhythmicity ± SEM	E-peak phase ± SEM	Free-running period ± SEM	Rhythmic power ± SEM
w^{1118} (male)	97.3 ± 2.66	11.92 ± 0.07	23.8 ± 0.04	97.8 ± 3.88
Pdf^{01} (male)	30.3 ± 5.05	11.72 ± 0.07	23.72 ± 0.13	22.1 ± 3.24
w^{1118} (female)	92.8 ± 3.27	11.71 ± 0.07	24.1 ± 0.04	109.9 ± 5.63
Pdf^{01} (female)	56.9 ± 3.63	11.85 ± 0.08	23.9 ± 0.09	49.63 ± 4

Table 2: Cosinor analysis parameters for *Canton-S* males and females.

Cosinor parameters for PDF cycling in s-LNv dorsal termini					
Genotype	p value	PR	Mesor ± s.e.	Amplitude ± s.e.	Phase ± s.e.
Canton-S (male)	2.02e−06	42.1	17.15 ± 2.67	22.38 ± 3.79	-4.71 ± 9.64
Canton-S (female)	7.33e−07	37.554	14.59 ± 2.9	24.47 ± 4.07	-19.13 ± 9.65

Table 3: Table representing the % rhythmicity, phase of the E-peak, free-running period and rhythmic power of w^{1118} and $PdfR^{01}$ males and females.

$PdfR^{01}$				
Genotype	% Rhythmicity ± SEM	E-peak phase ± SEM	Free-running period ± SEM	Rhythmic power ± SEM
w^{1118} (male)	97.3 ± 2.66	11.68 ± 0.07	23.8 ± 0.03	103.1 ± 4.15

PdfR^{01} (male)	16.4 ± 1.64	10.33 ± 0.04	21.8 ± 0.12	17.46 ± 2.28
w^{1118} (female)	92.7 ± 3.25	11.45 ± 0.07	24.1 ± 0.05	89.13 ± 4.75
PdfR^{01} (female)	65.4 ± 5.8	10.36 ± 0.07	22.4 ± 0.07	47.3 ± 3.5

Table 4: Table representing the % rhythmicity, % complex rhythms, free-running period and rhythmic power of *control and Pdf >* males and females.

Pdf > DBT^{s}				
Genotype	% Rhythmicity ± SEM	% Complex rhythms ± SEM	Free-running period ± SEM	Rhythmic power ± SEM
Pdf-Gal4 (male)	95.86 ± 2.73	0	24.3 ± 0.03	111.8 ± 5.58
UAS DBT^{s} (male)	96.79 ± 2.21	0	23.9 ± 0.01	134.8 ± 4.44
Pdf > DBT^{s} (male)	69.87 ± 6.89	23.73 ± 5.51	18.9 ± 0.14	49.48 ± 3.54
Pdf-Gal4 (female)	93.56 ± 4.02	0	24.4 ± 0.03	122 ± 6.76
UAS DBT^{s} (female)	89.45 ± 2.74	0	24.2 ± 0.03	89.7 ± 5.19
Pdf > DBT^{s} (female)	38.41 ± 2.74	5.54 ± 3.45	22.5 ± 0.58	24.8 ± 3.55

745 **References**
746
747 1. Anderson ST, FitzGerald GA. Sexual dimorphism in body clocks. Science.
748 2020;369(6508):1164-5. doi: doi:10.1126/science.abd4964.
749 2. Bailey M, Silver R. Sex differences in circadian timing systems: implications for disease. Front
750 Neuroendocrinol. 2014;35(1):111-39. Epub 2013/11/30. doi: 10.1016/j.yfrne.2013.11.003.
751 PubMed PMID: 24287074; PubMed Central PMCID: PMCPMC4041593.
752 3. Vida B, Hrabovszky E, Kalamatianos T, Coen CW, Liposits Z, Kalló I. Oestrogen Receptor α and
753 β Immunoreactive Cells in the Suprachiasmatic Nucleus of Mice: Distribution, Sex Differences
754 and Regulation by Gonadal Hormones. Journal of Neuroendocrinology. 2008;20(11):1270-7. doi:
755 https://doi.org/10.1111/j.1365-2826.2008.01787.x.
756 4. Lyall LM, Wyse CA, Graham N, Ferguson A, Lyall DM, Cullen B, et al. Association of disrupted
757 circadian rhythmicity with mood disorders, subjective wellbeing, and cognitive function: a cross-
758 sectional study of 91 105 participants from the UK Biobank. Lancet Psychiatry. 2018;5(6):507-
759 14. Epub 2018/05/20. doi: 10.1016/S2215-0366(18)30139-1. PubMed PMID: 29776774.
760 5. Bixler EO, Papaliaga MN, Vgontzas AN, Lin HM, Pejovic S, Karataraki M, et al. Women sleep
761 objectively better than men and the sleep of young women is more resilient to external
762 stressors: effects of age and menopause. J Sleep Res. 2009;18(2):221-8. Epub 2009/03/24. doi:
763 10.1111/j.1365-2869.2008.00713.x. PubMed PMID: 19302341; PubMed Central PMCID:
764 PMCPMC3594776.
765 6. Hastings MH, Maywood ES, Brancaccio M. The Mammalian Circadian Timing System and the
766 Suprachiasmatic Nucleus as Its Pacemaker. Biology (Basel). 2019;8(1). Epub 20190311. doi:
767 10.3390/biology8010013. PubMed PMID: 30862123; PubMed Central PMCID:
768 PMCPMC6466121.
769 7. Helfrich-Forster C. The neuroarchitecture of the circadian clock in the brain of Drosophila
770 melanogaster. Microsc Res Tech. 2003;62(2):94-102. Epub 2003/09/11. doi:
771 10.1002/jemt.10357. PubMed PMID: 12966496.
772 8. Schubert FK, Hagedorn N, Yoshii T, Helfrich-Forster C, Rieger D. Neuroanatomical details of
773 the lateral neurons of Drosophila melanogaster support their functional role in the circadian
774 system. J Comp Neurol. 2018;526(7):1209-31. Epub 2018/02/10. doi: 10.1002/cne.24406.
775 PubMed PMID: 29424420; PubMed Central PMCID: PMCPMC5873451.
776 9. Yu W, Hardin PE. Circadian oscillators of Drosophila and mammals. J Cell Sci. 2006;119(Pt
777 23):4793-5. Epub 2006/11/30. doi: 10.1242/jcs.03174. PubMed PMID: 17130292.
778 10. Kloss B, Price JL, Saez L, Blau J, Rothenfluh A, Wesley CS, et al. The Drosophila clock gene
779 double-time encodes a protein closely related to human casein kinase Iepsilon. Cell.
780 1998;94(1):97-107. Epub 1998/07/23. doi: 10.1016/s0092-8674(00)81225-8. PubMed PMID:
781 9674431.
782 11. Price JL, Blau J, Rothenfluh A, Abodeely M, Kloss B, Young MW. double-time is a novel
783 Drosophila clock gene that regulates PERIOD protein accumulation. Cell. 1998;94(1):83-95. Epub
784 1998/07/23. doi: 10.1016/s0092-8674(00)81224-6. PubMed PMID: 9674430.
785 12. Helfrich-Forster C. Organization of endogenous clocks in insects. Biochem Soc Trans.
786 2005;33(Pt 5):957-61. Epub 2005/10/26. doi: 10.1042/BST20050957. PubMed PMID: 16246020.

787 13. Ma D, Przybylski D, Abruzzi KC, Schlichting M, Li Q, Long X, et al. A transcriptomic
788 taxonomy of Drosophila circadian neurons around the clock. eLife. 2021;10:e63056. doi:
789 10.7554/eLife.63056.
790 14. Shafer OT, Helfrich-Forster C, Renn SC, Taghert PH. Reevaluation of Drosophila
791 melanogaster's neuronal circadian pacemakers reveals new neuronal classes. J Comp Neurol.
792 2006;498(2):180-93. Epub 2006/07/21. doi: 10.1002/cne.21021. PubMed PMID: 16856134;
793 PubMed Central PMCID: PMCPMC2596765.
794 15. Shafer OT, Gutierrez GJ, Li K, Mildenhall A, Spira D, Marty J, et al. Connectomic analysis of
795 the Drosophila lateral neuron clock cells reveals the synaptic basis of functional pacemaker
796 classes. Elife. 2022;11. Epub 2022/06/30. doi: 10.7554/eLife.79139. PubMed PMID: 35766361;
797 PubMed Central PMCID: PMCPMC9365390.
798 16. Grima B, Chelot E, Xia R, Rouyer F. Morning and evening peaks of activity rely on different
799 clock neurons of the Drosophila brain. Nature. 2004;431(7010):869-73. Epub 2004/10/16. doi:
800 10.1038/nature02935. PubMed PMID: 15483616.
801 17. Rieger D, Shafer OT, Tomioka K, Helfrich-Forster C. Functional analysis of circadian
802 pacemaker neurons in Drosophila melanogaster. J Neurosci. 2006;26(9):2531-43. Epub
803 2006/03/03. doi: 10.1523/JNEUROSCI.1234-05.2006. PubMed PMID: 16510731.
804 18. Renn SC, Park JH, Rosbash M, Hall JC, Taghert PH. A pdf neuropeptide gene mutation and
805 ablation of PDF neurons each cause severe abnormalities of behavioral circadian rhythms in
806 Drosophila. Cell. 1999;99(7):791-802. Epub 2000/01/05. PubMed PMID: 10619432.
807 19. Park JH, Helfrich-Forster C, Lee G, Liu L, Rosbash M, Hall JC. Differential regulation of
808 circadian pacemaker output by separate clock genes in Drosophila. Proc Natl Acad Sci U S A.
809 2000;97(7):3608-13. Epub 2000/03/22. doi: 10.1073/pnas.070036197. PubMed PMID:
810 10725392; PubMed Central PMCID: PMCPMC16287.
811 20. Stoleru D, Peng Y, Nawathean P, Rosbash M. A resetting signal between Drosophila
812 pacemakers synchronizes morning and evening activity. Nature. 2005;438(7065):238-42. Epub
813 2005/11/11. doi: 10.1038/nature04192. PubMed PMID: 16281038.
814 21. Stoleru D, Peng Y, Agosto J, Rosbash M. Coupled oscillators control morning and evening
815 locomotor behaviour of Drosophila. Nature. 2004;431(7010):862-8. Epub 2004/10/16. doi:
816 10.1038/nature02926. PubMed PMID: 15483615.
817 22. Fernandez MP, Pettibone HL, Bogart JT, Roell CJ, Davey CE, Pranevicius A, et al. Sites of
818 Circadian Clock Neuron Plasticity Mediate Sensory Integration and Entrainment. Curr Biol.
819 2020;30(12):2225-37 e5. Epub 2020/05/11. doi: 10.1016/j.cub.2020.04.025. PubMed PMID:
820 32386535; PubMed Central PMCID: PMCPMC7314648.
821 23. Guo F, Chen X, Rosbash M. Temporal calcium profiling of specific circadian neurons in
822 freely moving flies. Proc Natl Acad Sci U S A. 2017;114(41):E8780-E7. Epub 2017/10/05. doi:
823 10.1073/pnas.1706608114. PubMed PMID: 28973886; PubMed Central PMCID:
824 PMCPMC5642695.
825 24. Lamaze A, Stanewsky R. DN1p or the "Fluffy" Cerberus of Clock Outputs. Front Physiol.
826 2019;10:1540. Epub 2020/01/24. doi: 10.3389/fphys.2019.01540. PubMed PMID: 31969832;
827 PubMed Central PMCID: PMCPMC6960142.
828 25. Collins B, Kane Elizabeth A, Reeves David C, Akabas Myles H, Blau J. Balance of Activity
829 between LNvs and Glutamatergic Dorsal Clock Neurons Promotes Robust Circadian Rhythms in
830 Drosophila. Neuron. 2012;74(4):706-18. doi: https://doi.org/10.1016/j.neuron.2012.02.034.

26. Yoshii T, Wulbeck C, Sehadova H, Veleri S, Bichler D, Stanewsky R, et al. The neuropeptide pigment-dispersing factor adjusts period and phase of Drosophila's clock. J Neurosci. 2009;29(8):2597-610. Epub 2009/02/27. doi: 10.1523/JNEUROSCI.5439-08.2009. PubMed PMID: 19244536.
27. Peng Y, Stoleru D, Levine JD, Hall JC, Rosbash M. Drosophila free-running rhythms require intercellular communication. PLoS Biol. 2003;1(1):E13. Epub 2003/09/17. doi: 10.1371/journal.pbio.0000013. PubMed PMID: 12975658; PubMed Central PMCID: PMCPMC193604.
28. Liang X, Holy TE, Taghert PH. A Series of Suppressive Signals within the Drosophila Circadian Neural Circuit Generates Sequential Daily Outputs. Neuron. 2017;94(6):1173-89 e4. Epub 2017/05/30. doi: 10.1016/j.neuron.2017.05.007. PubMed PMID: 28552314; PubMed Central PMCID: PMCPMC5502710.
29. Mertens I, Vandingenen A, Johnson EC, Shafer OT, Li W, Trigg JS, et al. PDF receptor signaling in Drosophila contributes to both circadian and geotactic behaviors. Neuron. 2005;48(2):213-9. Epub 2005/10/26. doi: 10.1016/j.neuron.2005.09.009. PubMed PMID: 16242402.
30. Hyun S, Lee Y, Hong ST, Bang S, Paik D, Kang J, et al. Drosophila GPCR Han is a receptor for the circadian clock neuropeptide PDF. Neuron. 2005;48(2):267-78. Epub 2005/10/26. doi: 10.1016/j.neuron.2005.08.025. PubMed PMID: 16242407.
31. Lear BC, Merrill CE, Lin JM, Schroeder A, Zhang L, Allada R. A G protein-coupled receptor, groom-of-PDF, is required for PDF neuron action in circadian behavior. Neuron. 2005;48(2):221-7. Epub 2005/10/26. doi: 10.1016/j.neuron.2005.09.008. PubMed PMID: 16242403.
32. Kim WJ, Jan LY, Jan YN. A PDF/NPF neuropeptide signaling circuitry of male Drosophila melanogaster controls rival-induced prolonged mating. Neuron. 2013;80(5):1190-205. doi: 10.1016/j.neuron.2013.09.034. PubMed PMID: 24314729; PubMed Central PMCID: PMCPMC3867312.
33. Krupp JJ, Billeter JC, Wong A, Choi C, Nitabach MN, Levine JD. Pigment-dispersing factor modulates pheromone production in clock cells that influence mating in drosophila. Neuron. 2013;79(1):54-68. Epub 2013/07/16. doi: 10.1016/j.neuron.2013.05.019. PubMed PMID: 23849197; PubMed Central PMCID: PMCPMC3955580.
34. Inami S, Sato S, Kondo S, Tanimoto H, Kitamoto T, Sakai T. Environmental Light Is Required for Maintenance of Long-Term Memory in Drosophila. J Neurosci. 2020;40(7):1427-39. Epub 2020/01/15. doi: 10.1523/JNEUROSCI.1282-19.2019. PubMed PMID: 31932417; PubMed Central PMCID: PMCPMC7044726.
35. Toma DP, White KP, Hirsch J, Greenspan RJ. Identification of genes involved in Drosophila melanogaster geotaxis, a complex behavioral trait. Nat Genet. 2002;31(4):349-53. Epub 2002/06/04. doi: 10.1038/ng893. PubMed PMID: 12042820.
36. Guo F, Yu J, Jung HJ, Abruzzi KC, Luo W, Griffith LC, et al. Circadian neuron feedback controls the Drosophila sleep--activity profile. Nature. 2016;536(7616):292-7. Epub 2016/08/02. doi: 10.1038/nature19097. PubMed PMID: 27479324; PubMed Central PMCID: PMCPMC5247284.
37. Chen D, Sitaraman D, Chen N, Jin X, Han C, Chen J, et al. Genetic and neuronal mechanisms governing the sex-specific interaction between sleep and sexual behaviors in

874 Drosophila. Nat Commun. 2017;8(1):154. Epub 2017/07/30. doi: 10.1038/s41467-017-00087-5.
875 PubMed PMID: 28754889; PubMed Central PMCID: PMCPMC5533705.
876 38. Kunst M, Hughes ME, Raccuglia D, Felix M, Li M, Barnett G, et al. Calcitonin gene-related
877 peptide neurons mediate sleep-specific circadian output in Drosophila. Curr Biol.
878 2014;24(22):2652-64. Epub 2014/12/03. doi: 10.1016/j.cub.2014.09.077. PubMed PMID:
879 25455031; PubMed Central PMCID: PMCPMC4255360.
880 39. Helfrich-Forster C. Differential control of morning and evening components in the activity
881 rhythm of Drosophila melanogaster--sex-specific differences suggest a different quality of
882 activity. J Biol Rhythms. 2000;15(2):135-54. Epub 2000/04/13. doi:
883 10.1177/074873040001500208. PubMed PMID: 10762032.
884 40. Palmateer CM, Artikis C, Brovero SG, Friedman B, Gresham A, Arbeitman MN. Single-cell
885 transcriptome profiles of Drosophila fruitless-expressing neurons from both sexes. eLife.
886 2023;12:e78511. doi: 10.7554/eLife.78511.
887 41. Fujii S, Amrein H. Ventral lateral and DN1 clock neurons mediate distinct properties of
888 male sex drive rhythm in Drosophila. Proc Natl Acad Sci U S A. 2010;107(23):10590-5. Epub
889 2010/05/26. doi: 10.1073/pnas.0912457107. PubMed PMID: 20498055; PubMed Central
890 PMCID: PMCPMC2890825.
891 42. Hanafusa S, Kawaguchi T, Umezaki Y, Tomioka K, Yoshii T. Sexual interactions influence the
892 molecular oscillations in DN1 pacemaker neurons in Drosophila melanogaster. PLoS One.
893 2013;8(12):e84495. Epub 2013/12/25. doi: 10.1371/journal.pone.0084495. PubMed PMID:
894 24367668; PubMed Central PMCID: PMCPMC3867508.
895 43. Lee G, Bahn JH, Park JH. Sex- and clock-controlled expression of the neuropeptide F gene
896 in Drosophila. Proc Natl Acad Sci U S A. 2006;103(33):12580-5. Epub 20060807. doi:
897 10.1073/pnas.0601171103. PubMed PMID: 16894172; PubMed Central PMCID:
898 PMCPMC1567921.
899 44. Hermann C, Yoshii T, Dusik V, Helfrich-Forster C. Neuropeptide F immunoreactive clock
900 neurons modify evening locomotor activity and free-running period in Drosophila melanogaster.
901 J Comp Neurol. 2012;520(5):970-87. Epub 2011/08/10. doi: 10.1002/cne.22742. PubMed PMID:
902 21826659.
903 45. Nässel DR, Zandawala M. Recent advances in neuropeptide signaling in Drosophila, from
904 genes to physiology and behavior. Prog Neurobiol. 2019;179:101607. Epub 2019/03/25. doi:
905 10.1016/j.pneurobio.2019.02.003. PubMed PMID: 30905728.
906 46. Kuwano R, Katsura M, Iwata M, Yokosako T, Yoshii T. Pigment-dispersing factor and
907 CCHamide1 in the Drosophila circadian clock network. Chronobiol Int. 2023;40(3):284-99. Epub
908 2023/02/15. doi: 10.1080/07420528.2023.2166416. PubMed PMID: 36786215.
909 47. Parisky KM, Agosto J, Pulver SR, Shang Y, Kuklin E, Hodge JJ, et al. PDF cells are a GABA-
910 responsive wake-promoting component of the Drosophila sleep circuit. Neuron.
911 2008;60(4):672-82. Epub 2008/11/29. doi: 10.1016/j.neuron.2008.10.042. PubMed PMID:
912 19038223; PubMed Central PMCID: PMCPMC2734413.
913 48. Cornelissen G. Cosinor-based rhythmometry. Theoretical Biology and Medical Modelling.
914 2014;11(1):16. doi: 10.1186/1742-4682-11-16.
915 49. Im SH, Li W, Taghert PH. PDFR and CRY signaling converge in a subset of clock neurons to
916 modulate the amplitude and phase of circadian behavior in Drosophila. PLoS One.

917 2011;6(4):e18974. Epub 2011/05/12. doi: 10.1371/journal.pone.0018974. PubMed PMID:
918 21559487; PubMed Central PMCID: PMCPMC3084726.
919 50. Richhariya S, Shin D, Le JQ, Rosbash M. Dissecting neuron-specific functions of circadian
920 genes using modified cell-specific CRISPR approaches. Proc Natl Acad Sci U S A.
921 2023;120(29):e2303779120. Epub 2023/07/10. doi: 10.1073/pnas.2303779120. PubMed PMID:
922 37428902; PubMed Central PMCID: PMCPMC10629539.
923 51. Gorostiza EA, Ceriani MF. Retrograde Bone Morphogenetic Protein Signaling Shapes a Key
924 Circadian Pacemaker Circuit. The Journal of Neuroscience. 2013;33(2):687-96. doi:
925 10.1523/jneurosci.3448-12.2013.
926 52. Ruben M, Drapeau MD, Mizrak D, Blau J. A mechanism for circadian control of pacemaker
927 neuron excitability. J Biol Rhythms. 2012;27(5):353-64. doi: 10.1177/0748730412455918.
928 PubMed PMID: 23010658; PubMed Central PMCID: PMCPMC4019749.
929 53. Fleck SA, Biswas P, DeWitt ED, Knuteson RL, Eisman RC, Nemkov T, et al. Auxin Exposure
930 Disrupts Feeding Behavior and Fatty Acid Metabolism in Adult Drosophila. bioRxiv. 2023. Epub
931 2023/08/30. doi: 10.1101/2023.08.15.553385. PubMed PMID: 37645868; PubMed Central
932 PMCID: PMCPMC10462055.
933 54. McGuire SE, Mao Z, Davis RL. Spatiotemporal gene expression targeting with the TARGET
934 and gene-switch systems in Drosophila. Sci STKE. 2004;2004(220):pl6. Epub 2004/02/19. doi:
935 10.1126/stke.2202004pl6. PubMed PMID: 14970377.
936 55. Yao Z, Shafer OT. The Drosophila circadian clock is a variably coupled network of multiple
937 peptidergic units. Science. 2014;343(6178):1516-20. Epub 2014/03/29. doi:
938 10.1126/science.1251285. PubMed PMID: 24675961; PubMed Central PMCID:
939 PMCPMC4259399.
940 56. Muskus MJ, Preuss F, Fan J-Y, Bjes ES, Price JL. Drosophila DBT Lacking Protein Kinase
941 Activity Produces Long-Period and Arrhythmic Circadian Behavioral and Molecular Rhythms.
942 Molecular and Cellular Biology. 2007;27(23):8049-64. doi: 10.1128/mcb.00680-07.
943 57. Kaneko M, Park JH, Cheng Y, Hardin PE, Hall JC. Disruption of synaptic transmission or
944 clock-gene-product oscillations in circadian pacemaker cells of Drosophila cause abnormal
945 behavioral rhythms. J Neurobiol. 2000;43(3):207-33. Epub 2000/06/08. doi: 10.1002/(sici)1097-
946 4695(20000605)43:3<207::aid-neu1>3.0.co;2-0. PubMed PMID: 10842235.
947 58. Blanchardon E, Grima B, Klarsfeld A, Chelot E, Hardin PE, Preat T, et al. Defining the role of
948 Drosophila lateral neurons in the control of circadian rhythms in motor activity and eclosion by
949 targeted genetic ablation and PERIOD protein overexpression. Eur J Neurosci. 2001;13(5):871-
950 88. Epub 2001/03/27. doi: 10.1046/j.0953-816x.2000.01450.x. PubMed PMID: 11264660.
951 59. Umezaki Y, Yasuyama K, Nakagoshi H, Tomioka K. Blocking synaptic transmission with
952 tetanus toxin light chain reveals modes of neurotransmission in the PDF-positive circadian clock
953 neurons of Drosophila melanogaster. J Insect Physiol. 2011;57(9):1290-9. Epub 2011/06/29. doi:
954 10.1016/j.jinsphys.2011.06.004. PubMed PMID: 21708159.
955 60. Yao Z, Bennett AJ, Clem JL, Shafer OT. The Drosophila Clock Neuron Network Features
956 Diverse Coupling Modes and Requires Network-wide Coherence for Robust Circadian Rhythms.
957 Cell Rep. 2016;17(11):2873-81. Epub 2016/12/16. doi: 10.1016/j.celrep.2016.11.053. PubMed
958 PMID: 27974202; PubMed Central PMCID: PMCPMC5161247.
959 61. Brown MP, Verma S, Palmer I, Zuniga AG, Rosensweig C, Keles MF, et al. A subclass of
960 evening cells promotes the switch from arousal to sleep at dusk. bioRxiv. 2023. Epub

961 2023/09/11. doi: 10.1101/2023.08.28.555147. PubMed PMID: 37693540; PubMed Central
962 PMCID: PMCPMC10491161.
963 62. Delventhal R, O'Connor RM, Pantalia MM, Ulgherait M, Kim HX, Basturk MK, et al.
964 Dissection of central clock function in Drosophila through cell-specific CRISPR-mediated clock
965 gene disruption. Elife. 2019;8. Epub 2019/10/16. doi: 10.7554/eLife.48308. PubMed PMID:
966 31613218; PubMed Central PMCID: PMCPMC6794090.
967 63. Schlichting M, Diaz MM, Xin J, Rosbash M. Neuron-specific knockouts indicate the
968 importance of network communication to Drosophila rhythmicity. Elife. 2019;8. Epub
969 2019/10/16. doi: 10.7554/eLife.48301. PubMed PMID: 31613223; PubMed Central PMCID:
970 PMCPMC6794074.
971 64. Bulthuis N, Spontak KR, Kleeman B, Cavanaugh DJ. Neuronal Activity in Non-LNv Clock
972 Cells Is Required to Produce Free-Running Rest:Activity Rhythms in Drosophila. J Biol Rhythms.
973 2019;34(3):249-71. Epub 2019/04/18. doi: 10.1177/0748730419841468. PubMed PMID:
974 30994046; PubMed Central PMCID: PMCPMC7153773.
975 65. Shansky RM, Murphy AZ. Considering sex as a biological variable will require a global shift
976 in science culture. Nature Neuroscience. 2021;24(4):457-64. doi: 10.1038/s41593-021-00806-8.
977 66. Kokras N, Dalla C. Sex differences in animal models of psychiatric disorders. British Journal
978 of Pharmacology. 2014;171(20):4595-619. doi: https://doi.org/10.1111/bph.12710.
979 67. Beery AK, Zucker I. Sex bias in neuroscience and biomedical research. Neurosci Biobehav
980 Rev. 2011;35(3):565-72. Epub 2010/07/14. doi: 10.1016/j.neubiorev.2010.07.002. PubMed
981 PMID: 20620164; PubMed Central PMCID: PMCPMC3008499.
982 68. Joye DAM, Evans JA. Sex differences in daily timekeeping and circadian clock circuits.
983 Semin Cell Dev Biol. 2022;126:45-55. Epub 20210514. doi: 10.1016/j.semcdb.2021.04.026.
984 PubMed PMID: 33994299; PubMed Central PMCID: PMCPMC8589873.
985 69. Taghert PH, Nitabach MN. Peptide neuromodulation in invertebrate model systems.
986 Neuron. 2012;76(1):82-97. Epub 2012/10/09. doi: 10.1016/j.neuron.2012.08.035. PubMed
987 PMID: 23040808; PubMed Central PMCID: PMCPMC3466441.
988 70. Goda T, Umezaki Y, Alwattari F, Seo HW, Hamada FN. Neuropeptides PDF and DH31
989 hierarchically regulate free-running rhythmicity in Drosophila circadian locomotor activity.
990 Scientific Reports. 2019;9(1):838. doi: 10.1038/s41598-018-37107-3.
991 71. Helfrich-Forster C. Robust circadian rhythmicity of Drosophila melanogaster requires the
992 presence of lateral neurons: a brain-behavioral study of disconnected mutants. J Comp Physiol
993 A. 1998;182(4):435-53. Epub 1998/04/08. PubMed PMID: 9530835.
994 72. Fernandez MP, Berni J, Ceriani MF. Circadian remodeling of neuronal circuits involved in
995 rhythmic behavior. PLoS Biol. 2008;6(3):e69. Epub 2008/03/28. doi:
996 10.1371/journal.pbio.0060069. PubMed PMID: 18366255; PubMed Central PMCID:
997 PMCPMC2270325.
998 73. Biondi G, McCormick G, Fernandez MP. The Drosophila Circadian Clock Gene Cycle
999 Controls Development of Clock Neurons. bioRxiv. 2023:2023.10.29.564626. doi:
1000 10.1101/2023.10.29.564626.
1001 74. Sweeney ST, Broadie K, Keane J, Niemann H, O'Kane CJ. Targeted expression of tetanus
1002 toxin light chain in Drosophila specifically eliminates synaptic transmission and causes
1003 behavioral defects. Neuron. 1995;14(2):341-51. Epub 1995/02/01. doi: 10.1016/0896-
1004 6273(95)90290-2. PubMed PMID: 7857643.

1005 75. Kaneko M, Helfrich-Forster C, Hall JC. Spatial and temporal expression of the period and
1006 timeless genes in the developing nervous system of Drosophila: newly identified pacemaker
1007 candidates and novel features of clock gene product cycling. J Neurosci. 1997;17(17):6745-60.
1008 Epub 1997/09/01. PubMed PMID: 9254686.
1009 76. Hofbauer B, Zandawala M, Reinhard N, Rieger D, Werner C, Evers JF, et al. The
1010 neuropeptide pigment-dispersing factor signals independently of Bruchpilot-labelled active
1011 zones in daily remodelled terminals of Drosophila clock neurons. European Journal of
1012 Neuroscience. 2024;59(10):2665-85. doi: https://doi.org/10.1111/ejn.16294.
1013 77. Johard HAD, Yoishii T, Dircksen H, Cusumano P, Rouyer F, Helfrich-Förster C, et al.
1014 Peptidergic clock neurons in Drosophila: Ion transport peptide and short neuropeptide F in
1015 subsets of dorsal and ventral lateral neurons. Journal of Comparative Neurology.
1016 2009;516(1):59-73. doi: 10.1002/cne.22099.
1017 78. Todd WD, Fenselau H, Wang JL, Zhang R, Machado NL, Venner A, et al. A hypothalamic
1018 circuit for the circadian control of aggression. Nat Neurosci. 2018;21(5):717-24. Epub 20180409.
1019 doi: 10.1038/s41593-018-0126-0. PubMed PMID: 29632359; PubMed Central PMCID:
1020 PMCPMC5920747.
1021 79. Fujii S, Krishnan P, Hardin P, Amrein H. Nocturnal male sex drive in Drosophila. Curr Biol.
1022 2007;17(3):244-51. Epub 2007/02/06. doi: 10.1016/j.cub.2006.11.049. PubMed PMID:
1023 17276917; PubMed Central PMCID: PMCPMC2239012.
1024 80. Sakai T, Ishida N. Circadian rhythms of female mating activity governed by clock genes in
1025 Drosophila. Proc Natl Acad Sci U S A. 2001;98(16):9221-5. Epub 2001/07/27. doi:
1026 10.1073/pnas.151443298. PubMed PMID: 11470898; PubMed Central PMCID: PMCPMC55401.
1027 81. T M, Hari Dass S, Sharma VK. Egg-laying rhythm in Drosophila melanogaster. J Genet.
1028 2008;87(5):495-504. Epub 2009/01/17. doi: 10.1007/s12041-008-0072-9. PubMed PMID:
1029 19147938.
1030 82. Zhang C, Daubnerova I, Jang YH, Kondo S, Žitňan D, Kim YJ. The neuropeptide allatostatin C
1031 from clock-associated DN1p neurons generates the circadian rhythm for oogenesis. Proc Natl
1032 Acad Sci U S A. 2021;118(4). doi: 10.1073/pnas.2016878118. PubMed PMID: 33479181;
1033 PubMed Central PMCID: PMCPMC7848730.
1034 83. Persons JL, Abhilash L, Lopatkin AJ, Roelofs A, Bell EV, Fernandez MP, et al. PHASE: An
1035 Open-Source Program for the Analysis of DrosophilaPhase, Activity, and Sleep Under
1036 Entrainment. J Biol Rhythms. 2022;37(4):455-67. Epub 2022/06/22. doi:
1037 10.1177/07487304221093114. PubMed PMID: 35727044; PubMed Central PMCID:
1038 PMCPMC10362883.
1039 84. Schindelin J, Arganda-Carreras I, Frise E, Kaynig V, Longair M, Pietzsch T, et al. Fiji: an open-
1040 source platform for biological-image analysis. Nature Methods. 2012;9:676. doi:
1041 10.1038/nmeth.2019
1042 https://www.nature.com/articles/nmeth.2019#supplementary-information.
1043 85. Lee Gierke C, Cornelissen G. Chronomics analysis toolkit (CATkit). Biol Rhythm Res.
1044 2016;47(2):163-81. doi: 10.1080/09291016.2015.1094965.
1045

Figure 1

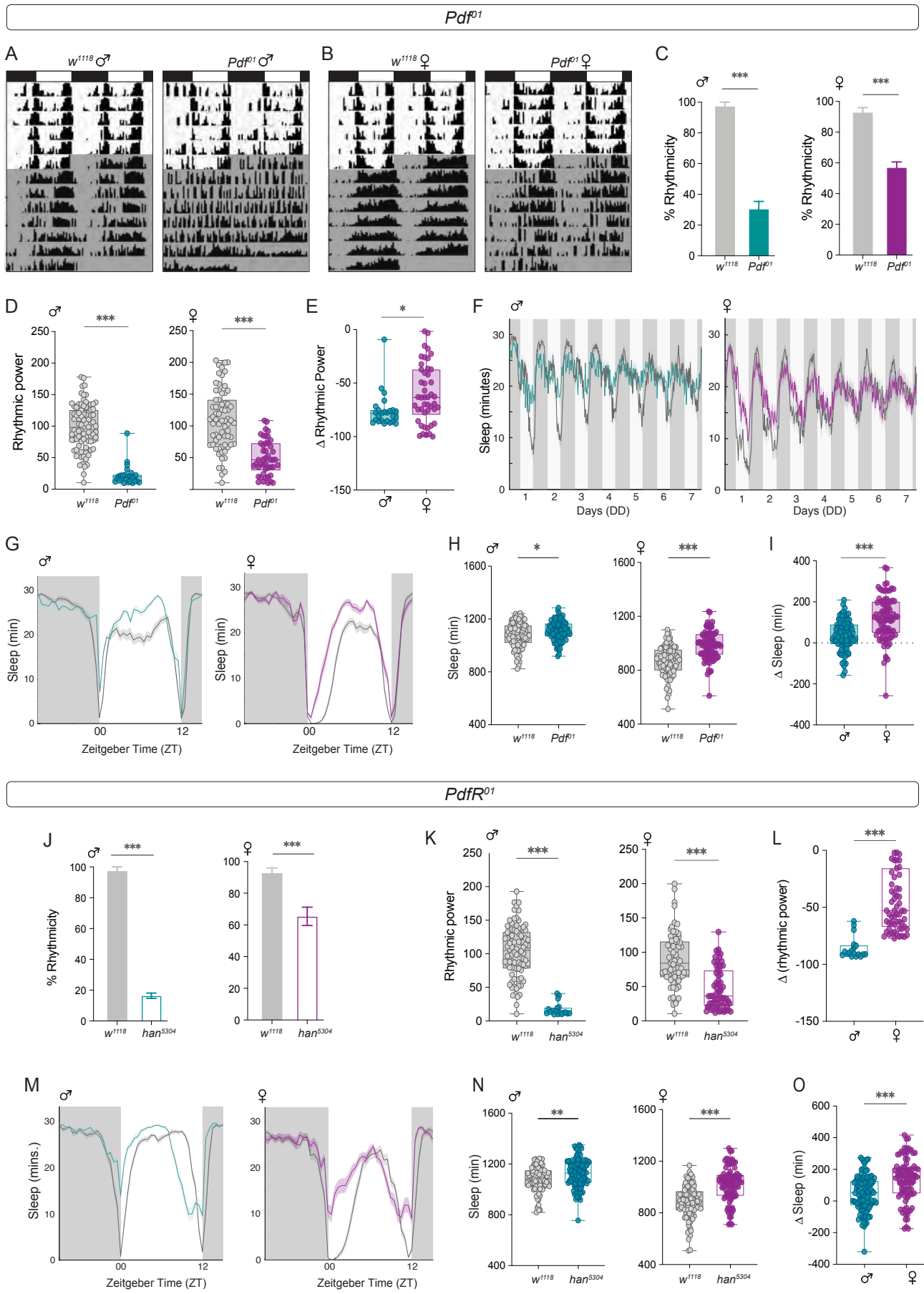
Pdf01
A
w1118 ♂
Pdf01 ♂
B
w1118 ♀
Pdf01 ♀
C
% Rhythmicity
D
Rhythmic power
E
Δ Rhythmic Power
F
Sleep (minutes)
Days (DD)
G
Sleep (min)
Zeitgeber Time (ZT)
H
Sleep (min)
I
Δ Sleep (min)
PdfR01
J
% Rhythmicity
K
Rhythmic power
L
Δ (rhythmic power)
M
Sleep (mins.)
Zeitgeber Time (ZT)
N
Sleep (min)
O
Δ Sleep (min)

Pdf > Cas9 + Pdf-g

A

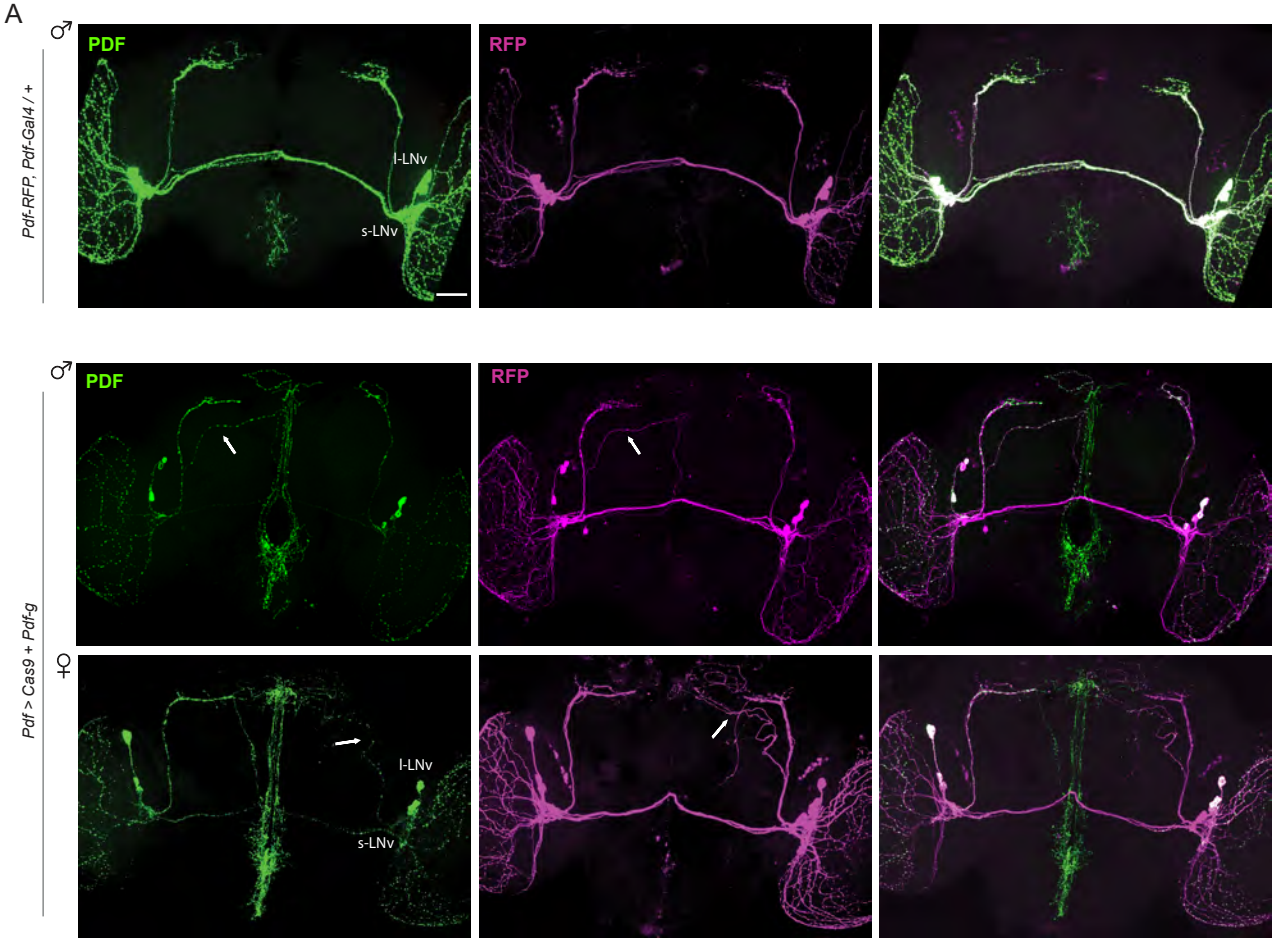

B

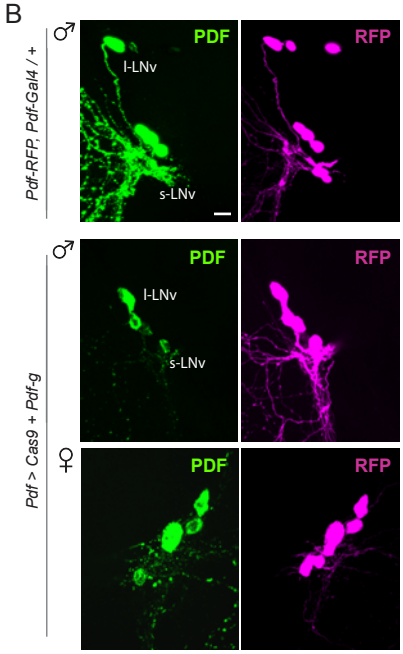

C

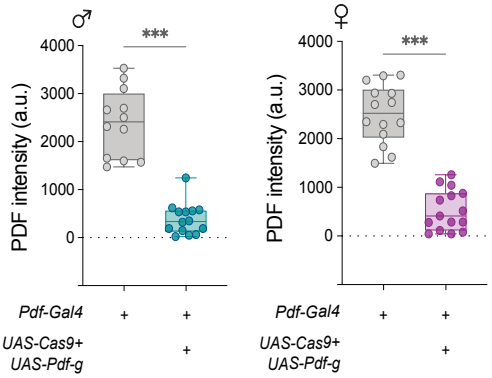

D

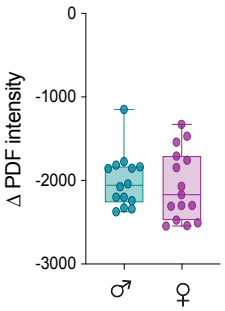

Figure 3

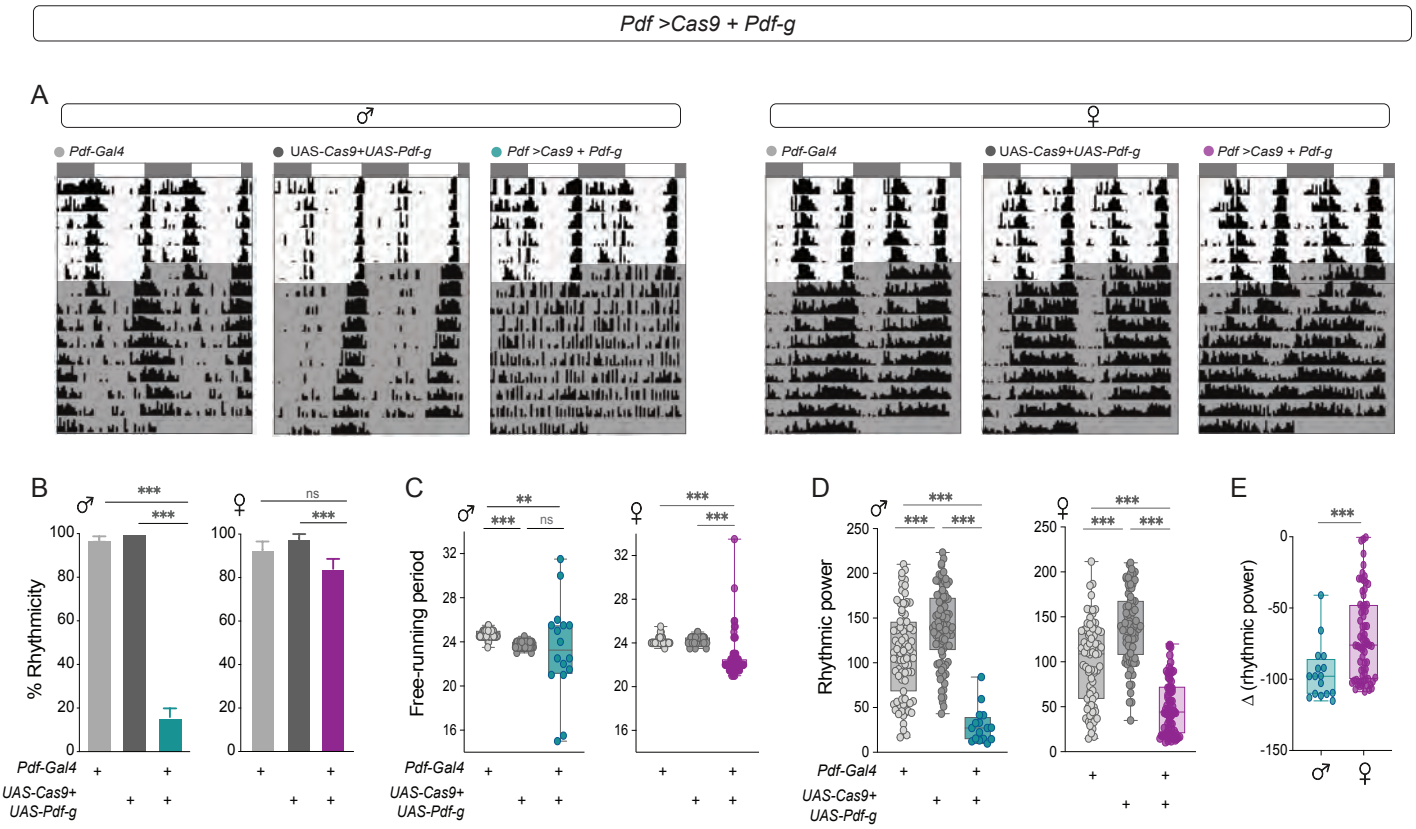
Pdf >Cas9 + Pdf-g
A
♂
♀
Pdf-Gal4
UAS-Cas9+UAS-Pdf-g
Pdf >Cas9 + Pdf-g
B
% Rhythmicity
C
Free-running period
D
Rhythmic power
E
Δ (rhythmic power)
Pdf-Gal4
UAS-Cas9+
UAS-Pdf-g
***
**
ns

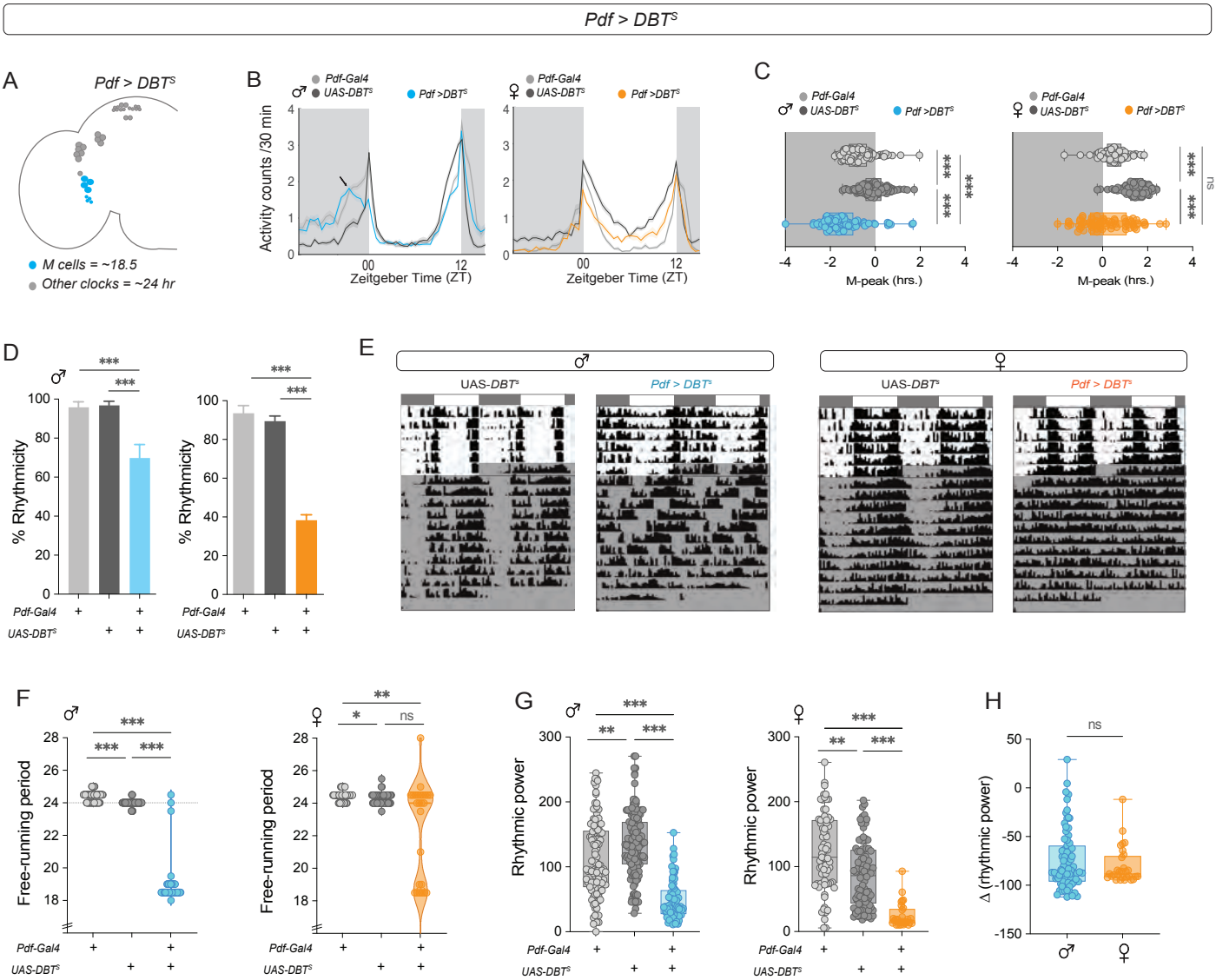
Pdf > DBTS
A
Pdf > DBTS
M cells = ~18.5
Other clocks = ~24 hr
B
Pdf-Gal4
UAS-DBTS
Pdf >DBTS
Activity counts /30 min
Zeitgeber Time (ZT)
C
M-peak (hrs.)
ns
D
% Rhythmicity
E
UAS-DBTS
Pdf > DBTS
F
Free-running period
G
Rhythmic power
H
Δ (rhythmic power)

Figure 5

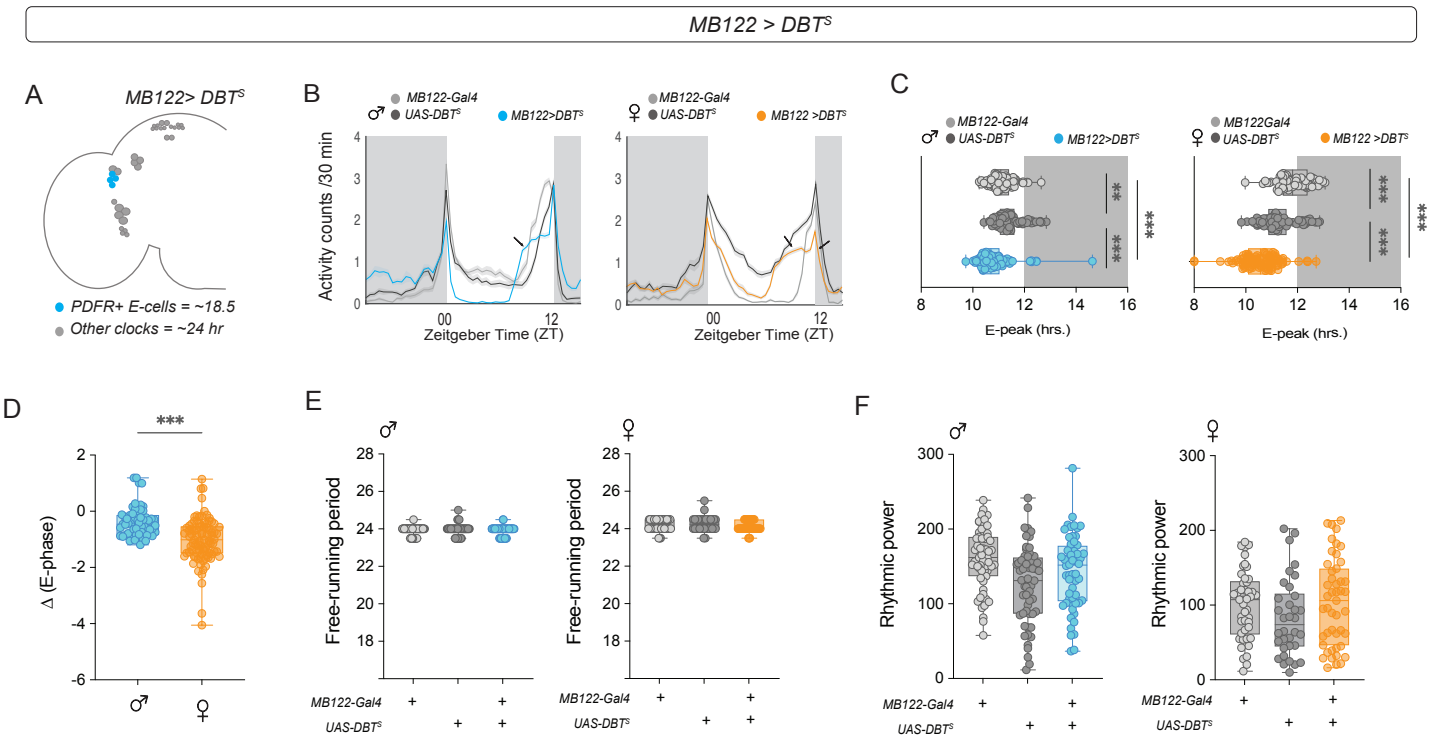
MB122 > DBTS
A
MB122> DBTS
PDFR+ E-cells = ~18.5
Other clocks = ~24 hr
B
MB122-Gal4
UAS-DBTS
MB122>DBTS
MB122 >DBTS
Activity counts /30 min
Zeitgeber Time (ZT)
C
E-peak (hrs.)
D
Δ (E-phase)
E
Free-running period
F
Rhythmic power